Generalized Eigenspaces and Pseudospectra of Nonnormal and Defective Matrix-Valued Dynamical Systems

Saori Morimoto, * Makoto Katori, † and Tomoyuki Shirai, ‡

3 December 2024

Abstract

We consider nonnormal matrix-valued dynamical systems with discrete time. For an eigenvalue of matrix, the number of times it appears as a root of the characteristic polynomial is called the algebraic multiplicity. On the other hand, the geometric multiplicity is the dimension of the linear space of eigenvectors associated with that eigenvalue. If the former exceeds the latter, then the eigenvalue is said to be defective and the matrix becomes nondiagonalizable by any similarity transformation. The discrete-time of our dynamics is identified with the geometric multiplicity of the zero eigenvalue $\lambda_0 = 0$. Its algebraic multiplicity takes about half of the matrix size at $t = 1$ and increases stepwise in time, which keeps excess to the geometric multiplicity until their coincidence at the final time. Our model exhibits relaxation processes from far-from-normal to near-normal matrices, in which the defectivity of λ_0 is recovering in time. We show that such processes are realized as size reductions of pseudospectrum including λ_0. Here the pseudospectra are the domains on the complex plane which are not necessarily exact spectra but in which the resolvent of matrix takes extremely large values. The defective eigenvalue λ_0 is sensitive to perturbation and the eigenvalues of the perturbed systems are distributed densely in the pseudospectrum including λ_0. By constructing generalized eigenspace for λ_0, we give the Jordan block decomposition for the resolvent of matrix and characterize the pseudospectrum dynamics. Numerical study of the systems perturbed by Gaussian random matrices supports the validity of the present analysis.

Keywords: Nonnormal matrices, Defective eigenvalue, Pseudospectrum dynamics, Generalized eigenspaces, Jordan decompositions of resolvents, Symbol curves

2020 Mathematics Subject Classification: 15A18; 15A20; 15B05; 47A10; 60B20

*Department of Physics, Faculty of Science and Engineering, Chuo University, Kasuga, Bunkyo-ku, Tokyo 112-8551, Japan

†Department of Physics, Faculty of Science and Engineering, Chuo University, Kasuga, Bunkyo-ku, Tokyo 112-8551, Japan; e-mail: makoto.katori.mathphys@gmail.com

‡Institute of Mathematics for Industry, Kyushu University, 744 Motooka, Nishi-ku, Fukuoka 819-0395, Japan; e-mail: shirai@imi.kyushu-u.ac.jp

1 Introduction

Consider a matrix $M \in \mathbb{C}^{n \times n}$. We write its Hermitian conjugate as $M^\dagger$ defined by the complex conjugate of the transpose; $M^\dagger := \overline{M^\mathsf{T}}$. If it satisfies the equality $M^\dagger M = M M^\dagger$, then it is said to be *normal* and can be diagonalized by a unitary transformation. Hermitian matrices satisfying $M^\dagger = M$ fall in this class. We introduce two notions of degeneracy of eigenvalues. The *algebraic multiplicity* is the number of times the eigenvalue appears as a root of the characteristic polynomial of M, while the *geometric multiplicity* is the dimension of the linear space of the eigenvectors associated to the eigenvalue. When the geometric multiplicity is equal to the algebraic multiplicity for all eigenvalues, the matrix M has a complete set of eigenvectors. In this case, even if M is nonnormal, it can be reduced to a diagonal matrix Λ by a similarity transformation as $\Lambda = V^{-1} M V$. Here the j-th column of V is given by the j-th linearly independent eigenvector, $j = 1, 2, \ldots, n$, and V^{-1} is well defined. But if the algebraic multiplicity of an eigenvalue exceeds the geometric multiplicity, then that eigenvalue is said to be *defective* and the matrix becomes nondiagoralizable.

Consider the *shift matrix* with size $n \geq 2$,

$$S = S_n := \left(\delta_{j\,k-1} \right)_{1 \leq j, k \leq n} = \begin{pmatrix} 0 & 1 & & & & \\ & 0 & 1 & & \text{\Large 0} & \\ & \cdots & \cdots & & & \\ & & \cdots & \cdots & & \\ & & & 0 & 1 & \\ & & & & 0 & 1 \\ \text{\Large 0} & & & & & 0 \end{pmatrix}, \tag{1.1}$$

where δ_{jk} denotes the Kronecker delta. It is obvious that $S^k = 0$ for $k \geq n$. Let $b_j \in \mathbb{C}$, $j = 1, 2, \ldots$, and consider *nilpotent Toeplitz matrices*,

$$S(m) := S^m + b_1 S^{m+1} + \cdots + b_{n-m-1} S^{n-1}, \tag{1.2}$$

for $m = 1, 2, \ldots, n - 1$. Notice that $S(m)$, $m = 1, 2, \ldots, n - 1$ are non-Hermitian and nonnormal. Since all the elements of the diagonal and lower triangular part of $S(m)$ are zero,

$$\lambda_0 := 0$$

is the only eigenvalue. Hence, the algebraic multiplicity of λ_0, which is denoted by $a_0(m)$, is n for any $m = 1, 2, \ldots, n - 1$. For each $m = 1, 2, \ldots, n - 1$, any vector $\boldsymbol{v}_0(m)$ in the form $\boldsymbol{v}_0(m) = (v_{01}(m), v_{02}(m), \cdots, v_{0m}(m), 0, \cdots, 0)^\mathsf{T}$ can be an eigenvector for λ_0. The dimension of the complex space spanned by these eigenvectors is m. Hence the geometric multiplicity $g_0(m)$ of λ_0 is m. We notice that $g_0(1) = a_0(1) = 1$, but

$$g_0(m) < a_0(m), \quad m = 2, 3, \ldots, n - 1.$$

That is, the eigenvectors fail to span $\mathbb{C}^n$. In this case, the eigenvalue λ_0 is defective and there is no similarity transformation which reduces $S(m)$ to any diagonal form.

Although $S(m)$ is nondiagonalizable, a similarity transformation can reduce the matrix to the *Jordan canonical form*,

$$\mathbb{J}(m) = V(m)^{-1} S(m) V(m).$$

The diagonal elements of $\mathbb{J}(m)$ are still all zero, but some of the upper 2nd-diagonal elements can be 1. More precisely, $\mathbb{J}(m)$ is decomposed into $g_0(m)$-ple *Jordan blocks* which are given by shift matrices (1.1),

$$\mathbb{J}(m) = \bigoplus_{\ell=1}^{g_0(m)} S_{d_0^{(\ell)}(m)}, \tag{1.3}$$

where the sizes of them are denoted by $d_0^{(\ell)}(m)$, $\ell = 1, 2, \ldots, g_0(m)$. By convention, we assume the non-increasing order, $d_0^{(1)}(m) \geq d_0^{(2)}(m) \geq \cdots \geq d_0^{(g_0(m))}(m)$. Each $d_0^{(\ell)}(m)$ gives the dimension of the *generalized sub-eigenspace* which includes the ℓ-th eigenvector $\boldsymbol{v}_0^{(\ell)}(m)$ associated with the zero-eigenvalue λ_0, $\ell = 1, 2, \ldots, g_0(m)$. They satisfy the sum rule $\sum_{\ell=1}^{g_0(m)} d_0^{(\ell)}(m) = a_0(m)$. By definition, if $d_0^{(\ell)} \equiv 1$, $\ell = 1, 2, \ldots, g_0$, then $g_0 = a_0$ and the matrix is normal. Therefore,

$$k_0(m) := \max\{d_0^{(\ell)}(m) : \ell = 1, 2, \ldots, g_0(m)\} = d_0^{(1)}(m) \tag{1.4}$$

will indicate the degree of defectivity of the zero-eigenvalue λ_0 measuring how far from being normal. It is called the *index* of λ_0.

Eigenvalue analysis is one of the most successful method of applied mathematics. Roughly speaking, eigenvalues give us the abstraction of a matrix by plotting the set of them (*spectra*) on a complex plane $\mathbb{C}$. For defective matrices, however, eigenvalue analysis fails. In the above case with $S(m)$, the unique eigenvalue at zero with full algebraic multiplicity $a_0(m) \equiv n$ misleads us to identify $S(m)$ with the null (all-zero) matrix O. The Jordan-block structure with zero diagonal can not be represented only by spectra.

The structure of $S(m)$ hidden in eigenvalue analysis is revealed by its sensitivity to perturbation. Let $Z = (Z_{jk})_{1 \leq j, k \leq n}$ be a matrix consisting of independently and normally distributed complex entries;

$$Z_{jk} = X_{jk} + i Y_{jk} \quad \text{with} \quad X_{jk} \sim \mathrm{N}(0, 1), \quad Y_{jk} \sim \mathrm{N}(0, 1), \tag{1.5}$$

where $i := \sqrt{-1}$. Here we consider a simple case for (1.2) such that $b_1 = b \in \mathbb{C}$, $b_j = 0$ for $j \geq 2$. Figure 1a shows plots of the numerically obtained eigenvalues, when the complex Gaussian random matrix Z is added,

$$S^{(b)}(m, \widetilde{\delta} Z) := S^m + b S^{m+1} + \widetilde{\delta} Z, \tag{1.6}$$

where $n = 5000$, $m = 3$, $b = 1$, and the coefficient of Z is given by $\widetilde{\delta} = \widetilde{\delta}(n) = 1/\sqrt{2n} = 1/100$. The dots are not the eigenvalues of the original matrix, $S^{(b)}(m, 0) = S^m + b S^{m+1}$, but they represent the structure of this defective matrix in the sense explained below. Hence they are called the *pseudo-eigenvalues* of $S^{(b)}(m, 0)$. (More precisely speaking, the domains

3
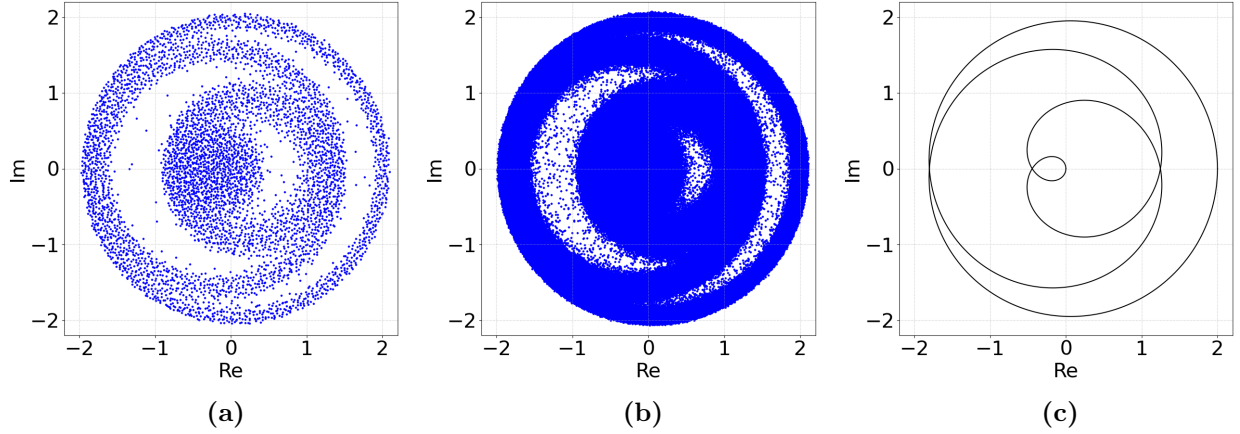
Figure 1: (a) One sampling result of numerically obtained eigenvalues of the system with Gaussian perturbation matrix Z; $S^{(b)}(m, \delta Z) = S^m + bS^{m+1} + (1/\sqrt{2n})Z$, where $n = 5000$, $m = 3$, and $b = 1$. (b) Superpositions of 50 samples. (c) Symbol curve of $\widehat{S}^m + b\widehat{S}^{m+1}$ with $m = 3$ and $b = 1$.

on $\mathbb{C}$ in which the eigenvalues of randomly perturbed matrix are distributed are called the *pseudospectra* of the original unperturbed matrix having defective eigenvalues [6, 23, 26].)
Instead of the $n \times n$ shift matrix (1.1), here we consider an infinite-size shift matrix,

$$\widehat{S} := S_\infty = (\delta_{j\,k-1})_{1 \le j,k < \infty}. \tag{1.7}$$

which will represent a *nilpotent Toeplitz operator*. We also consider an infinite-dimensional vector $\widehat{\boldsymbol{v}}$ in the form $\widehat{\boldsymbol{v}} = (1, z, z^2, z^3, \cdots)^\mathsf{T}$, $z \in \mathbb{C}$. Then we see that

$$(\widehat{S}^m + b\widehat{S}^{m+1})\widehat{\boldsymbol{v}} = f(z)\widehat{\boldsymbol{v}} \quad \text{with} \quad f(z) = z^m + bz^{m+1}. \tag{1.8}$$

The 2-norm of $\widehat{\boldsymbol{v}}$, $\|\widehat{\boldsymbol{v}}\| := (\sum_{j=1}^\infty |\widehat{v}_j|^2)^{1/2} = (1 - |z|^2)^{-1/2}$, is finite if z is inside the unit circle $\mathbb{T} := \{z \in \mathbb{C} : |z| = 1\}$. The function $f(z)$ is known as the *symbol* of the Toeplitz operator $\widehat{S}^m + b\widehat{S}^{m+1}$. The image of $\mathbb{T}$ by the map f, $f(\mathbb{T})$, is called the *symbol curve* of $\widehat{S}^m + b\widehat{S}^{m+1}$ and is drawn in Fig.1c for $b = 1$ [6, 26]. In Fig.1a, the plots of eigenvalues of the perturbed systems line up along the symbol curve $f(\mathbb{T})$. For all $z \in \mathbb{C}$, $|z| < 1$, the vectors $\widehat{\boldsymbol{v}}$ satisfying (1.8) give eigenvectors of eigenvalues $f(z) = z^m + bz^{m+1}$, $m - 1, 2, \ldots, n - 1$ in ℓ^2-space. It is proved that the spectrum of the Toeplitz operator $\widehat{S}^m + b\widehat{S}^{m+1}$ is equal to $f(\mathbb{T})$ with all the points enclosed by this curve (see, [23, Theorem 2.1], [26, Theorem 7.1]), and Section 5 (i) below). If numerically obtained eigenvalues of (1.6) were all superposed, they will fulfill the region bounded by the outmost curve of the symbol curve $f(\mathbb{T})$. Figure 1b shows superposition of the plots of 50 samples. Mathematical study of random perturbations of banded Toeplitz matrices, see [1, 2, 3, 4, 5, 24] and references therein.

Recently, the notion of pseudospectra has attracted much attention in stochastic analysis of time-dependent random matrix theory [13, 20]. The non-Hermitian matrix-valued

4

Brownian motion (BM) is defined by

$$M(t) = (M_{jk}(t))_{1 \le j,k \le n} := \left(\frac{1}{\sqrt{2n}} (B_{jk}^{\mathrm{R}}(t) + iB_{jk}^{\mathrm{I}}(t)) \right)_{1 \le j,k \le n}, \quad t \ge 0,$$

where $(B_{jk}^{\mathrm{R}}(t))_{t \ge 0}$, $(B_{jk}^{\mathrm{I}}(t))_{t \ge 0}$, $1 \le j, k \le n$ are $2n^2$ independent one-dimensional standard BMs [7, 8, 9, 12, 15, 18]. This process is regarded as the dynamical extension of the complex Ginibre ensemble, since if it starts from the null matrix, $M(0) = O$, the distribution of eigenvalues at an arbitrary time $t > 0$ is identified with the *complex Ginibre ensemble* of eigenvalues with variance t [17], which has been extensively studied in random matrix theory [10, 13]. Burda et al. [9] studied the process $(M(t))_{t \ge 0}$ starting from $M(0) = S$. By numerical simulation they found that the eigenvalues seem to expand instantly from λ_0 to a unit circle $\mathbb{T}$. For the time interval $0 < t < 1$, the dots form a growing annulus. Then the inner radius of the annulus shrinks to zero at $t = 1$ and dots fill up a full unit disk. This observation shall be compared with the eigenvalues of the matrix (1.6) with $m = 1$ and $b = 0$, where perturbation was given by a Gaussian complex random-matrix Z. When $m = 1$ and $b = 0$, the symbol is $f(z) = z$ and hence the symbol curve is simply a unit circle, $f(\mathbb{T}) = \mathbb{T}$. The transition from a unit circle to a unit disk in the time period $t \in (0, 1]$ reported by Burda et al. [9] will be regarded as a sampling process of eigenvalues for the perturbed nilpotent Toeplitz matrix. They seem to cluster along the symbol curve $\mathbb{T}$ when the sampling number is small, while they tend to fill the unit disk as the sampling number becomes large.

Motivated by the above consideration, we will study the following matrix-valued dynamical system [21],

$$S^{(b)}(t, \delta J) := S^{t+1} + bS^{t+2} + \delta J, \tag{1.9}$$

with discrete time $t = 0, 1, \ldots, T$, where the final time is defined by

$$T = T(n) := n - 2.$$

Here $b, \delta \in \mathbb{C}$ and J is the all-ones matrix; $J = (J_{jk})_{1 \le j,k \le n}$ with

$$J_{jk} \equiv 1, \quad j, k = 1, 2, \ldots n,$$

which gives the additive *rank 1 perturbation* [14] to the nilpotent Toeplitz matrices, $S^{(b)}(t, 0) = S^{t+1} + bS^{t+2}$.

We will show the following.

(i)   The discrete time t is equal to the geometric multiplicity of λ_0,

$$g_0(t) = t, \quad t = 0, 1, \ldots, T. \tag{1.10}$$

(See Proposition 3.1 in Section 3.1.) In other words, we consider the matrix-valued dynamical system such that the dimension of the eigenspace in the narrow sense associated with λ_0 is growing in time.

5
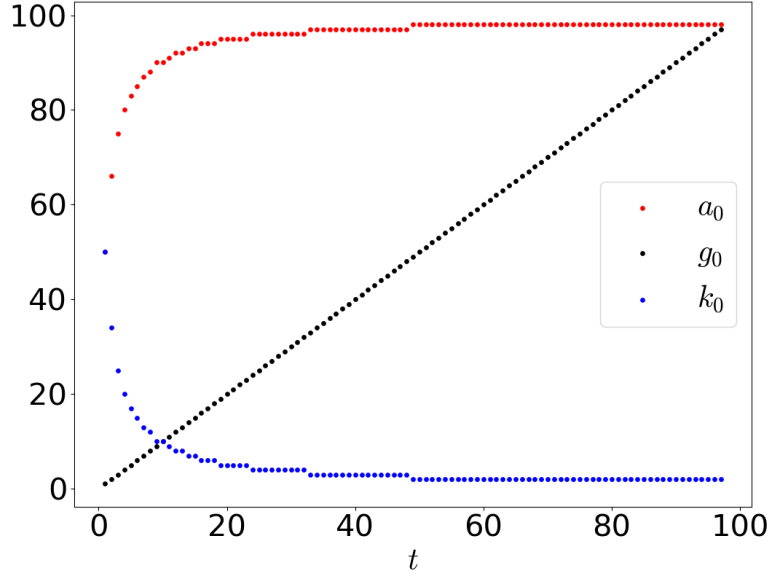
Figure 2: Time-evolution of the geometric multiplicity g_0, the algebraic multiplicity a_0, and the degree k_0 of λ_0 are shown by black, red, and blue dots, respectively, for $t = 1, 2, \ldots, T :=$ $n - 2$ with $n = 100$.

(ii) All non-zero eigenvalues of $S^{(b)}(t, \delta J)$ are given by simple roots of a polynomial equation with degree $p_1(t) + 1$ with

$$p_1(t) := \left\lfloor \frac{n-1}{t+1} \right\rfloor, \tag{1.11}$$

where $\lfloor x \rfloor$ denotes the greatest integer less than or equal to $x \in \mathbb{R}$ (the floor function of x) [21]. This determines the algebraic multiplicity of λ_0 as

$$a_0(t) = n - p_1(t) - 1, \quad t = 0, 1, \ldots, T. \tag{1.12}$$

(See Theorem 2.1 in Section 2.) Note that with a fixed n, $a_0(t)$ is increasing stepwise in t [21]. Notice that $a_0(0) = 0$; that is, the origin is not an eigenvalue at $t = 0$. When the origin becomes an eigenvalue at $t = 1$, its algebraic multiplicity has a large value $\lfloor n/2 \rfloor$, that is, approximately half of the matrix size n, while the system has only one $(g_0(1) = 1)$ eigenvector. Non-zero eigenvalues are being absorbed one by one to the origin [21], and the algebraic multiplicity $a_0(t)$ increases stepwise in time. The speed of increment of $a_0(t)$ is slowing down as t increases, but it keeps excess to $g_0(t)$ until $t = n - 3$. At the final time $t = T$, λ_0 has $a_0(T) = n - 2 = T$ leaving only two non-zero eigenvalues on $\mathbb{C}$. There are $g_0(T) = T$ linearly independent eigenvalues at that time. The coincidence $a_0(T) = g_0(T)$ makes the matrix be diagonalizable.

6
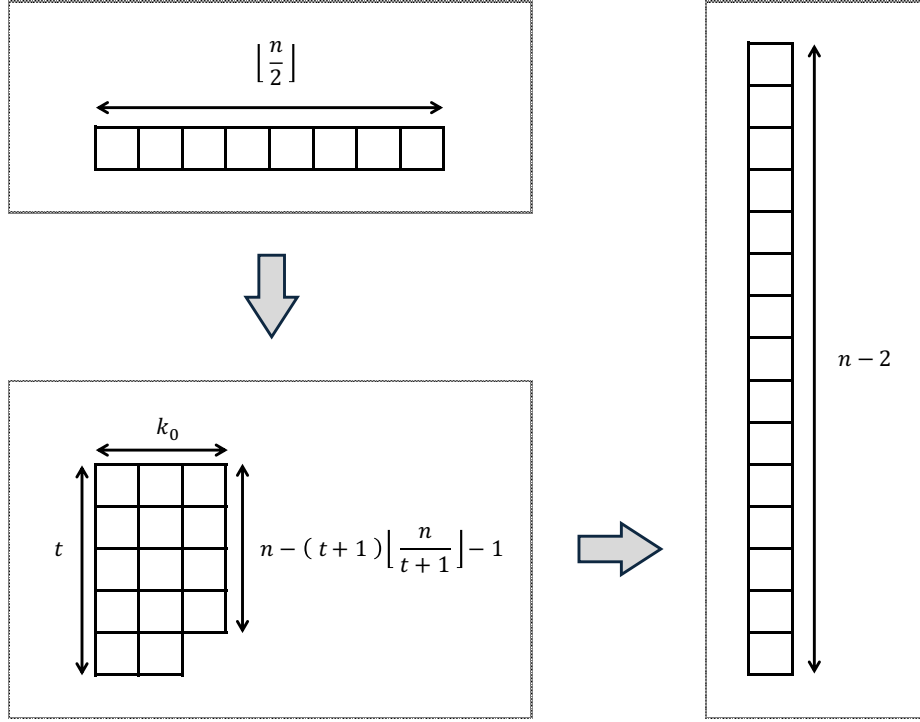
Figure 3: Time evolution of Young diagram representing the dynamics of the Jordan canonical form associated with λ_0. The upper-left diagram is for the initial time $t = 1$ with $\lfloor n/2 \rfloor$ boxes and the right diagram is for the final time $t = T$ with $n - 2$ boxes. Here we have drawn the case with $n = 17$. The lower-left diagram shows the intermediate state at time $t = 5$. In this case $n = 17$ is indivisible by $t + 1 = 6$; $(t + 1) \nmid n$. Then $k_0 = \lfloor n/(t + 1) \rfloor + 1 = 3$, $n - (t + 1)\lfloor n/(t + 1) \rfloor - 1 = 4$.

(iii) Although $g_0(0) = a_0(0) = 0$ and $g_0(T) = a_0(T) = T$, the inequality holds as

$$g_0(t) < a_0(t), \quad t = 1, 2, \ldots, T - 1.$$

That is, the matrices $S^{(b)}(t, \delta J)$ are nonnormal and λ_0 is defective. We will construct the generalized eigenspaces associated with λ_0 explicitly and prove that the *index* of λ_0 is given by

$$k_0(t) = \begin{cases} \dfrac{n}{t + 1}, & \text{if } (t + 1) \mid n, \\[3mm] \left\lfloor \dfrac{n}{t + 1} \right\rfloor + 1, & \text{if } (t + 1) \nmid n, \end{cases} \tag{1.13}$$

where $(t + 1) \mid n$ (resp. $(t + 1) \nmid n$) means that n is divisible (resp. indivisible) by $t + 1$. (See Proposition 3.2 in Section 3.1.) The degree of nonnormality is the highest

value at the beginning; $k_0(1) = n/2$ if n is even and $k_0(1) = (n+1)/2$ if n is odd. The defectivity of λ_0 is then decreasing stepwise in time. We put $k_0(T) = 1$ by convention. See Fig.2

(iv) At each time $t = 1, 2, \ldots, T - 1$, by a similarity transformation, $S^{(b)}(t, \delta J)$ is reduced to the following form,

$$\mathbb{J}(t) \oplus \mathrm{diag}(\lambda_1(t), \lambda_2(t), \ldots, \lambda_{p_1(t)+1}), \qquad (1.14)$$

where the Jordan canonical form $\mathbb{J}(t)$ is decomposed into t-ple Jordan blocks as

$$\mathbb{J}(t) = \begin{cases} \underbrace{S_{k_0(t)} \oplus \cdots \oplus S_{k_0(t)}}_{t}, & \text{if } (t+1) \mid n, \\ \underbrace{S_{k_0(t)} \oplus \cdots \oplus S_{k_0(t)}}_{n-(t+1)\lfloor n/(t+1)\rfloor -1} \oplus \underbrace{S_{k_0(t)-1} \oplus \cdots \oplus S_{k_0(t)-1}}_{t-n+(t+1)\lfloor n/(t+1)\rfloor +1}, & \text{if } (t+1) \nmid n. \end{cases} \qquad (1.15)$$

(See Section 3.1.) The Jordan canonical form is represented by a *Young diagram* [11, 16]. Figure 3 shows dynamics of Young diagram corresponding to (1.15). It starts from a single row diagram with $\lfloor n/2 \rfloor$ boxes at time $t = 1$ and ends with a single column diagram with $n - 2$ boxes at time $t = T$. (As mentioned at the end of (ii) above, at the final time $t = T$, $S^{(b)}(T, \delta J) = S^{n-1} + \delta J$ can be diagonalized into the form, $\mathrm{diag}(\underbrace{0, \cdots, 0}_{T}, \lambda_1(T), \lambda_2(T))$, $|\lambda_1(T)| > |\lambda_2(T)| > 0$ instead of (1.14).) The time t is identified with the number of rows and the total number of boxes is given by $a_0(t)$ which increases stepwise in time. The relaxation process of the defectivity of λ_0 is represented by the stepwise decreasing of the number of columns.

In summary, the present dynamical systems $(S^{(b)}(t, \delta J))_{1 \leq t \leq T}$, $b, \delta \in \mathbb{C}$, represent relaxation processes of matrices from being far-from-normal to being near-normal, in which the defective eigenvalue λ_0 is recovering in time. The paper is organized as follows. In Section 2 we derive the polynomial equation for the non-zero eigenvalues and discuss their time-evolution. Section 3 is devoted to the analytical study of the pseudospectra, in particular, the pseudospectrum including the defective eigenvalue $\lambda_0 = 0$. In Section 3.1 we explain how to construct the generalized eigenspace associated with λ_0, which is decomposed into t sub-spaces and gives the t-ple Jordan blocks for the similarity transformation of the matrix at each time t, We perform the Jordan decomposition of resolvent of the matrix, introduce the notion of generalized condition number, and then evaluate the 2-norm of the resolvent (Proposition 3.6) in Section 3.2. In Section 3.3, we give the first definition of ε-pseudospectrum (Definition 3). Then an estimation of the ε-pseudospectra is given by Theorem 3.8. This theorem clarifies the (t, n)-dependence of the pseudospectrum including λ_0. In order to show the validity of our analytical study, we perform numerical calculation for the processes perturbed by Gaussian complex random matrices in Section 4. In Section 4.1, we show the second definition of ε-pseudospectrum (Definition 4.1) which is equivalent with the first one. By this definition, the pseudospectrum is characterized by the sensitivity

8

of λ_0 with respect to perturbations. Actually, we show in Section 4.2, that (t, n)-dependence of the domain, in which the eigenvalues of the perturbed systems are accumulated, is consistent with Theorem 3.8 for the pseudospectrum including λ_0. Finally in Section 5 future problems are listed out.

2   Eigenvalue Dynamics

For the matrix-valued dynamical system $(S^{(b)}(t, \delta J))_{0 \le t \le T}$ given by (1.9), we consider the following eigenvalue and right-eigenvector equations,

$$S^{(b)}(t, \delta J)\boldsymbol{v}(t) = \lambda(t)\boldsymbol{v}(t), \quad t = 0, 1, \ldots, T, \tag{2.1}$$

$\boldsymbol{v}(t) = (v_1(t), \cdots, v_n(t))^{\mathsf{T}} \in \mathbb{C}^n$. Let $\boldsymbol{1}$ be the all-ones vector and we introduce the Hermitian inner product,

$$\langle \boldsymbol{u}, \boldsymbol{v} \rangle := \sum_{j=1}^{n} u_j \overline{v_j} = \boldsymbol{u}^{\mathsf{T}} \overline{\boldsymbol{v}}, \quad \boldsymbol{u}, \boldsymbol{v} \in \mathbb{C}^n. \tag{2.2}$$

Define

$$\alpha(\boldsymbol{v}) := \langle \boldsymbol{v}, \boldsymbol{1} \rangle = \sum_{j=1}^{n} v_j. \tag{2.3}$$

By definition, we have the equality

$$J\boldsymbol{v} = \alpha(\boldsymbol{v})\boldsymbol{1}. \tag{2.4}$$

We set $z = \lambda(t)$. Then (2.1) is written as

$$\{zI - (S^{t+1} + bS^{t+2})\}\boldsymbol{v}(t) = \delta\alpha(\boldsymbol{v}(t))\boldsymbol{1}. \tag{2.5}$$

If we consider the zero-eigenvalue $z = \lambda(t) = 0$, (2.5) becomes $-(S^{t+1} + bS^{t+2})\boldsymbol{v}(t) = \delta\alpha(\boldsymbol{v}(t))\boldsymbol{1}$. Since S^{t+1} and S^{t+2} shift the elements of any vector upward by $t+1$ and $t+2$ respectively when $S^{t+1} + bS^{t+2}$ is operated on the vector from the left, the last $t+1$ elements of the vector $-(S^{t+1} + bS^{t+2})\boldsymbol{v}(t)$ are zero. Since $\boldsymbol{1}$ is the all-ones vector, $\alpha(\boldsymbol{v}(t))$ should be 0. For non-zero eigenvalues $z = \lambda(t) \ne 0$ on the other hand, we can assume $\alpha(\boldsymbol{v}(t)) \ne 0$.

Let $1_{(\omega)}$ be the indicator function of the condition ω; $1_{(\omega)} = 1$ if ω is satisfied, and $1_{(\omega)} = 0$ otherwise. Remember that $p_1(t)$ is given by (1.11) and put

$$p_2(t) := \left\lfloor \frac{n-1}{t+2} \right\rfloor. \tag{2.6}$$

Theorem 2.1 *For $t = 0, 1, \ldots, T$, the following holds.*

9

(i) *There are $p_1(t) + 1$ non-zero eigenvalues, which solve equation,*

$$\frac{1+b}{n\delta}\left(\frac{z}{1+b}\right)^{p_1+1} - \frac{1 - \left(\frac{z}{1+b}\right)^{p_1+1}}{1 - \frac{z}{1+b}}$$

$$+ \left\{\frac{t+1}{n} + \frac{b}{(1+b)n}\right\}\frac{1}{1 - \frac{z}{1+b}}\left\{p_1 + 1 - \frac{1 - \left(\frac{z}{1+b}\right)^{p_1+1}}{1 - \frac{z}{1+b}}\right\}$$

$$- 1_{(p_1 \geq p_2+1,\, p_1 \geq (n+1)/(t+2))}\frac{1}{(1+b)^{p_1}}\sum_{k=0}^{p_1-p_2-1} z^k \sum_{q=n-(t+1)(p_1-k)+1}^{p_1-k} a^q \binom{p_1-k}{q}$$

$$\times \frac{1}{n}[q - \{n - (t+1)(p_1-k)\}] = 0. \quad (2.7)$$

This equation is also written as the polynomial equation,

$$\left(\frac{z}{1+b}\right)^{p_1(t)+1} - \frac{n\delta}{1+b}\sum_{k=0}^{p_1(t)}\left[1 - (p_1(t) - k)\left\{\frac{t+1}{n} + \frac{b}{(1+b)n}\right\}\right]\left(\frac{z}{1+b}\right)^k$$

$$- 1_{(p_1(t) \geq p_2(t)+1,\, p_1(t) \geq (n+1)/(t+2))}\frac{n\delta}{(1+b)^{p_1(t)+1}}$$

$$\times \sum_{k=0}^{p_1(t)-p_2(t)-1} z^k \sum_{q=n-m(p_1(t)-k)+1}^{p_1(m)-k} b^q\binom{p_1(t)-k}{q}\frac{1}{n}[q - \{n - (t+1)(p_1(t)-k)\}] = 0.$$

$$(2.8)$$

The corresponding right-eigenvectors $\boldsymbol{v}(t)$ satisfy $\alpha(\boldsymbol{v}(t)) \neq 0$.

(ii) *All other $n - p_1(t) - 1$ eigenvalues degenerate at zero. That is, the algebraic multiplicity of the zero eigenvalue, $\lambda_0 = 0$ is given by*

$$a_0(t) = n - p_1(t) - 1. \quad (2.9)$$

In this case, the corresponding right-eigenvectors $\boldsymbol{v}(t)$ satisfy $\alpha(\boldsymbol{v}(t)) = 0$, that is, they are orthogonal to $\boldsymbol{1}$.

Proof We solve (2.5) as follows,

$$\boldsymbol{v}(t) = \delta\alpha(\boldsymbol{v}(t))\{zI - (S^{t+1} + bS^{t+2})\}^{-1}\boldsymbol{1}$$

$$= \delta\alpha(\boldsymbol{v}(t))\sum_{k=0}^{\infty} z^{-(k+1)}(S^{t+1} + bS^{t+2})^k\boldsymbol{1}$$

$$= \delta\alpha(\boldsymbol{v}(t))\sum_{k=0}^{\infty} z^{-(k+1)}\sum_{q=0}^{k}\binom{k}{q}b^q S^{(t+1)k+q}\boldsymbol{1},$$

10

where we used the expansion formula of an inverse matrix. By taking inner products with **1** on both sides, we have

$$\langle \boldsymbol{v}(t), \mathbf{1}\rangle = \delta\alpha(\boldsymbol{v}(t)) \sum_{k=0}^{\infty} z^{-(k+1)} \sum_{q=0}^{k} \binom{k}{q} b^q \langle S^{(t+1)k+q}\mathbf{1}, \mathbf{1}\rangle.$$

Using the fact $\langle \boldsymbol{v}(t), \mathbf{1}\rangle = \alpha(v(t))$ and the equality

$$\langle S^\ell \mathbf{1}, \mathbf{1}\rangle = (n-\ell)1_{(1\le\ell\le n-1)}$$

for $S = S_n$, we arrive at the equality,

$$\alpha(\boldsymbol{v}(t)) = \delta\alpha(\boldsymbol{v}(t)) \sum_{k=0}^{p_1} z^{-(k+1)} \sum_{q=0}^{k} \binom{k}{q} b^q \Big[n - \{(t+1)k+q\}\Big] 1_{(1\le(t+1)k+q\le n-1)}.$$

For non-zero eigenvalues, we can assume $\alpha(\boldsymbol{v}(t)) \neq 0$. Then we have

$$\frac{1}{n\delta} - \sum_{k=0}^{p_1} z^{-(k+1)} \sum_{q=0}^{k} \binom{k}{q} b^q \left\{1 - \left(\frac{t+1}{n}k + \frac{q}{n}\right)\right\} 1_{(1\le(t+1)k+q\le n-1)} = 0.$$

The condition $(t+1)k+q \le n-1$ gives $q \le n-1-(t+1)k$. We see that for $n \in \mathbb{N}$,

$$k \le n-1-(t+1)k, \quad t \in \{2,3,\dots\}, k \in \mathbb{N}_0 := \{0,1,\dots\} \quad \Longleftrightarrow \quad k \le p_2, \quad k \in \mathbb{N}_0$$

where p_2 is defined by (2.6). That is, if $k \ge p_2 + 1$, then the summation over q is taken only in the interval $q \in [0, n-1-(t+1)k]$ instead of $[0, (t+1)k]$. In other words, in the index space $(k,q) \in \mathbb{N}_0 \times \mathbb{N}_0$, the region for which we should take summation is

$$\{(k,q); 1 \le k \le p_2, 0 \le q \le k\} \cup \{(k,q); p_2 + 1 \le k \le p_1, 0 \le q \le n-1-(t+1)k\}.$$

This is equivalent with

$$\{(k,q); 1 \le k \le p_1, 1 \le q \le k\} \setminus \{(k,q); p_2 + 1 \le k \le p_1, n-(t+1)k \le q \le k\}.$$

Hence the above equation is written as

$$\frac{1}{n\delta} - \sum_{k=0}^{p_1} z^{-(k+1)} \sum_{q=0}^{k} \binom{k}{q} b^q \left\{1 - \left(\frac{t+1}{n}k + \frac{q}{n}\right)\right\}$$

$$+ \sum_{k=p_2+1}^{p_1} z^{-(k+1)} \sum_{q=n-(t+1)k}^{k} \binom{k}{q} b^q \left\{1 - \left(\frac{t+1}{n}k + \frac{q}{n}\right)\right\} = 0. \tag{2.10}$$

We notice that

$$I_1(k) := \sum_{q=0}^{k} \binom{k}{q} b^q \left\{1 - \left(\frac{t+1}{n}k + \frac{q}{n}\right)\right\} = \left(1 - \frac{t+1}{n}k\right) \sum_{q=0}^{k} \binom{k}{q} b^q - \frac{1}{n} \sum_{q=0}^{k} q \binom{k}{q} b^q$$

$$= \left(1 - \frac{t+1}{n}k\right)(1+b)^k - \frac{1}{n}bk(1+b)^{k-1} = (1+b)^k - \frac{1}{n}\frac{(1+b)(t+1)+b}{1+b}k(1+b)^k,$$

and hence

$$J_1 := \sum_{k=0}^{p_1} z^{-(k+1)} I_1(k)$$

$$= (1+b)^{-1} \left(\frac{z}{1+b}\right)^{-1} \sum_{k=0}^{p_1} \left(\frac{z}{1+b}\right)^{-k}$$

$$- \frac{1}{n} \frac{(1+b)(t+1)+b}{1+b} (1+b)^{-1} \left(\frac{z}{1+b}\right)^{-1} \sum_{k=0}^{p_1} k \left(\frac{z}{1+b}\right)^{-k}.$$

It is easy to verify that this is written as

$$J_1 = \frac{1}{1+b} \left(\frac{z}{1+b}\right)^{-(p_1+1)} \frac{1 - \left(\frac{z}{1+b}\right)^{p_1+1}}{1 - \frac{z}{1+b}}$$

$$- \frac{1}{n} \frac{(1+b)(t+1)+b}{(1+b)^2} \frac{\left(\frac{z}{1+b}\right)^{-(p_1+1)}}{1 - \frac{z}{1+b}} \left\{ p_1 + 1 - \frac{1 - \left(\frac{z}{1+b}\right)^{p_1+1}}{1 - \frac{z}{1+b}} \right\}.$$

We also see that

$$J_2 := \sum_{k=p_2+1}^{p_1} z^{-(k+1)} \sum_{q=n-(t+1)k}^{k} b^q \binom{k}{q} b^q \left\{ 1 - \left(\frac{t+1}{n}k + \frac{q}{n}\right) \right\}$$

$$= - \left(\frac{z}{1+b}\right)^{-(p_1+1)} \frac{1}{(1+b)^{p_1+1}} \sum_{k=p_2+1}^{p_1} z^{p_1-k} \sum_{q=n-(t+1)k+1}^{k} b^q \binom{k}{q} \frac{1}{n} \{q - (n-(t+1)k)\}$$

$$= - \left(\frac{z}{1+b}\right)^{-(p_1+1)} \frac{1}{(1+b)^{p_1+1}} \sum_{\ell=0}^{p_1-p_2-1} z^\ell$$

$$\times \sum_{q=n-(t+1)(p_1-\ell)+1}^{p_1-\ell} b^q \binom{p_1-\ell}{q} \frac{1}{n} [q - \{n-(t+1)(p_1-\ell)\}],$$

where we have noticed that the term with $q = n - (t+1)k$ vanishes in the first line, and then the summation over k is replaced by the summation over $\ell := p_1 - k$ in the last line. J_2 should be zero if $p_1 = p_2$. For $0 \le \ell \le p_1 - p_2 - 1$, $n - (t+1)p_1 + 1 \le n - (t+1)(p_1 - \ell) + 1 \le q \le p_1 - \ell \le p_1$ in the second summation in the last line. Hence, if $n - (t+1)p_1 + 1 > p_1 \iff p_1 < (n+1)/(t+1+1)$, then J_2 should be zero. Equation (2.10) is thus given by

$$\frac{1}{n\delta} - J_1 + 1_{(p_1 \ge p_2+1, \, p_1 \ge (n+1)/(t+2))} J_2 = 0.$$

12

Multiply the factor $(1 + b) \times (z/(1 + b))^{p_1+1}$. Then (2.7) is obtained. It is easy to show that this equation is also written as (2.8). ∎

Remark 2.2 *The last term in the left-hand side of (2.8) will vanish or will be reduced into only one term if $n \geq \lceil n - 1 \rceil$, where $\lceil x \rceil$ denotes the smallest integer greater than or equal to $x \in \mathbb{R}$ (the ceiling function of x). The following is verified [21, Lemma 3.6]. Let $I_{n-1} := [\lceil \sqrt{n-1} \rceil, n - 1] \cap \mathbb{N}$ and $T_{n-1} := \{\lfloor (n-1)/k \rfloor; k = 1, 2, \ldots, n - 1\}$. Then*

$$p_1(t) - p_2(t) = \begin{cases} 1, & \text{if } t + 1 \in I_{n-1} \cap T_{n-1}, \\ 0, & \text{if } t + 1 \in I_{n-1} \setminus T_{n-1}. \end{cases}$$

Moreover, when $b = 0$, (2.8) is reduced to much simpler form as

$$z^{p_1(t)+1} - n\delta \sum_{k=0}^{p_1(t)} \left\{ 1 - (p_1(t) - k)\frac{t+1}{n} \right\} z^k = 0. \tag{2.11}$$

The following were proved as corollaries of Theorem 2.1 in [21].

Proposition 2.3 *There is an outlier eigenvalue $\lambda_1(t)$, whose modulus goes to ∞ as $n\delta \to \infty$. For $n\delta > 1$, we have the expression*

$$\lambda_1(t) = n\delta + 1 + b - (1 + b) \sum_{k=0}^{p_1(t)-1} C_k \left(\frac{t+1}{n} + \frac{b}{(1+b)n} \right)^{k+1} \left(\frac{1+b}{n\delta} \right)^k + O((n\delta)^{-p_1(t)})$$

$$+ 1_{(p_1(t) \geq p_2(t)+1)} O((n\delta)^{-p_2(t)}), \tag{2.12}$$

where C_k is the Catalan number; $C_k := \dfrac{1}{k+1} \dbinom{2k}{k} = \dfrac{(2k)!}{(k+1)!k!}, \; k \in \mathbb{N}_0$.

Proposition 2.4 *Fix δ and b. Consider t satisfying $\delta > 4\{(1 + b)(t + 1) + b\}/n^2$ and $p_1(t) = p_2(t)$. Then as $n \to \infty$, $p_1(t)$ non-zero eigenvalues except the outlier eigenvalue $\lambda_1(t)$ tend to form a configuration such that one point at $z = 1 + b$ is eliminated from the equidistance $p_1(t) + 1$ points on a circle centered the origin with radius $1 + b$;*

$$(1 + b)e^{2\pi i \ell/(p_1(t)+1)}, \quad \ell = 0, 1, \ldots, p_1(t).$$

For *outliers in spectra* discussed in random matrix theory, see [14, 25].

For the non-zero eigenvalues $\lambda_j(t)$, $j = 1, 2, \ldots, p_1(t) + 1$, the right- and left-eigenvectors are denoted by $\boldsymbol{v}_j(t)$ and $\boldsymbol{w}_j(t)$, respectively, $t = 0, 1, \ldots, T$. They are determined to satisfy the *bi-orthogonality relation*,

$$\langle \boldsymbol{w}_j(t), \boldsymbol{v}_k(t) \rangle = \delta_{j,k}, \quad j, k = 1, 2, \ldots, p_1(t) + 1, \quad t = 0, 1, \ldots, T. \tag{2.13}$$

3 Pseudospectrum Dynamics

3.1 Generalized eigenspaces associated with $\lambda_0 = 0$

The eigenvalue and right-eigenvector equations (2.1) with (1.9),

$$(S^{t+1} + bS^{t+2} + \delta J)\boldsymbol{v}(t) = \lambda(t)\boldsymbol{v}(t),$$

is written as

$$(S^{t+1} + bS^{t+2})\boldsymbol{v}(t) = \lambda(t)\boldsymbol{v}(t) - \delta\alpha(\boldsymbol{v}(t))\mathbf{1},$$

where $\alpha(\boldsymbol{v}(t))$ was defined by (2.3) and we have used the equality (2.4). We consider the right-eigenvectors $\boldsymbol{v}_0(t)$ associated with the zero-eigenvalue $\lambda(t) \equiv \lambda_0 = 0$;

$$(S^{t+1} + bS^{t+2})\boldsymbol{v}_0(t) = -\delta\alpha(\boldsymbol{v}_0(t))\mathbf{1}, \quad t = 1, 2, \ldots, T.$$

Let $\boldsymbol{e}_j := (\underbrace{0, \cdots, 0}_{j-1}, 1, \underbrace{0, \cdots, 0}_{n-j})^{\mathsf{T}} \in \mathbb{C}^n$ be the j-th standard vector, $j = 1, 2, \ldots, n$, and $V_k := \mathrm{span}\{\boldsymbol{e}_1, \boldsymbol{e}_2, \ldots, \boldsymbol{e}_k\}$, $k = 1, 2, \ldots, n$. Since S^{t+1} and S^{t+2} are upward shift operators for vectors by $t+1$ and $t+2$, respectively, $(S^{t+1} + bS^{t+2})\boldsymbol{u} \in V_{n-(t+1)}$ for any $\boldsymbol{u} \in \mathbb{C}^n$. On the other hand, $\mathbf{1}$ is the all-ones vector in V_n, and hence, $\mathbf{1} \notin V_{n-(t+1)}$. Therefore, $\alpha(\boldsymbol{v}_0(t)) = 0$ is concluded. The right-eigenvectors $\boldsymbol{v}_0(t) = (v_{01}(t), \ldots, v_{0n}(t))^{\mathsf{T}}$ for λ_0 are hence the solutions of the equations

$$(S^{t+1} + bS^{t+2})\boldsymbol{v}_0(t) = 0, \tag{3.1}$$

$$\sum_{j=1}^{n} v_{0j}(t) = 0, \quad t = 1, 2, \ldots, T. \tag{3.2}$$

Proposition 3.1 *The geometric multiplicity of λ_0 is given by*

$$g_0(t) = t. \tag{3.3}$$

Proof It is easy to verify that all the vectors satisfying (3.1) are in V_{t+1}. Since the zero-sum condition (3.2) is imposed for $v_{0j} \in \mathbb{C}, j = 1, \ldots, t+1$, the dimension of complex right-eigenvectors $\boldsymbol{v}_0$ is equal to t. The proof is complete. ∎

At each time $t = 1, 2, \ldots, T$, we write the t linearly independent solutions of (3.1) with (3.2) as $\boldsymbol{v}_0^{(\ell,1)}(t)$, $\ell = 1, 2, \ldots, t$. We choose the following solutions,

$$\boldsymbol{v}_0^{(\ell,1)}(t) = \boldsymbol{e}_1 - \boldsymbol{e}_{\ell+1} = \Big(1, \underbrace{0, \cdots, 0}_{\ell-1}, -1, \underbrace{0, \cdots, 0}_{n-(\ell+1)}\Big)^{\mathsf{T}} \in V_{\ell+1} \subset V_{t+1}. \tag{3.4}$$

Assume that $t = 1, 2, \ldots, T - 1$. For each right-eigenvector $\boldsymbol{v}_0^{(\ell,1)}(t)$, $\ell = 1, 2, \ldots, t$, the *generalized right-eigenvectors*, $\boldsymbol{v}_0^{(\ell,q)}(t)$, are given by the solutions of the *Jordan chain*,

$$(S^{t+1} + bS^{t+2} + \delta J)\boldsymbol{v}_0^{(\ell,q)}(t) = \boldsymbol{v}_0^{(\ell,q-1)}(t)$$

$$\iff \quad (S^{t+1} + bS^{t+2})\boldsymbol{v}_0^{(\ell,q)}(t) = \boldsymbol{v}_0^{(\ell,q-1)}(t) - \delta\alpha(\boldsymbol{v}_0^{(\ell,q)})\mathbf{1}, \quad q = 2, 3, \ldots. \tag{3.5}$$

Since $(S^{t+1} + bS^{t+2})\boldsymbol{v}_0^{(\ell,q)}(t) \in V_{n-(t+1)}$ in general, $\boldsymbol{v}_0^{(\ell,1)}(t) \in V_{t+1}$ implies $\alpha(\boldsymbol{v}_0^{(\ell,2)})$ multiplied by $\mathbf{1}$ should be zero. By reduction with respect to q, we show that the Jordan chain (3.5) is equivalent with

$$(S^{t+1} + bS^{t+2})\boldsymbol{v}_0^{(\ell,q)}(t) = \boldsymbol{v}_0^{(\ell,q-1)}(t), \tag{3.6}$$

$$\sum_{j=1}^{n} v_{0j}^{(\ell,q)}(t) = 0, \quad q = 2, 3, \ldots. \tag{3.7}$$

The dimension of the generalized ℓ-th sub-eigenspace denoted by $d_0^{(\ell)}(t)$ is the highest value of q satisfying (3.6) and (3.7) with non-zero $\boldsymbol{v}_0^{(\ell,q)}(t)$. We put

$$k_0(t) := \max_{\ell : 1 \leq \ell \leq t} d_0^{(\ell)}(t), \quad t = 1, 2, \ldots, T.$$

Proposition 3.2 *Assume that $t = 1, 2, \ldots, T - 1$.*

(i) *When $(t + 1) \mid n$,*
$$d_0^{(\ell)}(t) = \frac{n}{t + 1}, \quad \ell = 1, 2, \ldots, t. \tag{3.8}$$

Hence
$$k_0(t) = \frac{n}{t + 1}.$$

(ii) *When $(t + 1) \nmid n$, let $\xi := n \bmod (t + 1) \in \{1, 2, \ldots, t\}$. Then*

$$d_0^{(\ell)}(t) = \begin{cases} \left\lfloor \dfrac{n}{t + 1} \right\rfloor + 1, & 1 \leq \ell < \xi, \\[3mm] \left\lfloor \dfrac{n}{t + 1} \right\rfloor, & \xi \leq \ell \leq t. \end{cases} \tag{3.9}$$

Hence
$$k_0(t) = \left\lfloor \frac{n}{t + 1} \right\rfloor + 1.$$

Proof First consider (3.6) for $q = 2$. Since $S^{t+1} + bS^{t+2} = (I + bS)S^{t+1}$, and $I + bS$ is invertible, we have
$$S^{t+1}\boldsymbol{v}_0^{(\ell,2)}(t) = (I + bS)^{-1}\boldsymbol{v}_0^{(\ell,1)}(t). \tag{3.10}$$
For $\boldsymbol{u} = (u_1, \ldots, u_n)^{\mathsf{T}} \in V_n$, we define
$$S^{-(t+1)}\boldsymbol{u} = (\underbrace{0, \cdots, 0}_{t+1}, u_1, u_2, \ldots, u_{n-(t+1)})^{\mathsf{T}}. \tag{3.11}$$

Then (3.10) is solved by
$$\boldsymbol{v}_0^{(\ell,2)}(t) = \boldsymbol{u}_1 + \boldsymbol{u}_2, \tag{3.12}$$

15

where $\boldsymbol{u}_1$ is an arbitrary vector in V_{t+1} and $\boldsymbol{u}_2 := S^{-(t+1)}(I + bS)^{-1}\boldsymbol{v}_0^{(\ell,1)}(t)$. By the fact $\boldsymbol{v}_0^{(\ell,1)}(t) \in V_{\ell+1}$, we see that

$$(I + bS)^{-1}\boldsymbol{v}_0^{(\ell,1)}(t) = \sum_{k=0}^{\ell}(-b)^\ell S^\ell \boldsymbol{v}_0^{(\ell,1)}(t) \in V_{\ell+1}.$$

Hence, $\boldsymbol{v}_0^{(\ell,2)}(t) \in V_{(t+1)+(\ell+1)}$ is written in the form

$$\boldsymbol{v}_0^{(\ell,2)}(t) = (u_{11}, \ldots, u_{1\,t+1}, u_{21}, \ldots, u_{2\,\ell+1}, \underbrace{0, \cdots, 0}_{n-(t+1)-(\ell+1)})^\mathsf{T},$$

provided $\ell + 1 \leq n - (t+1)$. Finally, $\boldsymbol{u}_1 = (u_{11}, \ldots, u_{1\,t+1}, \underbrace{0, \cdots, 0}_{n-(t+1)})^\mathsf{T} \in V_{t+1}$ is chosen to satisfy $\alpha(\boldsymbol{u}_1) = -\alpha(\boldsymbol{u}_2)$, that is, to satisfy the zero-sum condition (3.7) for $q = 2$. One possibility is that

$$\boldsymbol{u}_1 = -\alpha(\boldsymbol{u}_2)\boldsymbol{e}_1 \in V_1. \tag{3.13}$$

By the same procedure, we can determine $\boldsymbol{v}_0^{(\ell,q)}(t) \in V_{(q-1)(t+1)+(\ell+1)}$ from $\boldsymbol{v}_0^{(\ell,q-1)}(t) \in V_{(q-2)(t+1)+(\ell+1)}$ for $q = 2, 3, \ldots, d_0^{(\ell)}(t)$, where $d_0^{(\ell)}(t)$ is given by (3.8) if $(t+1) \mid n$, and by (3.9) if $(t+1) \nmid n$ with $\xi := n \bmod (t+1)$, respectively. The proof is complete. ∎

Next we consider the left-eigenvectors for λ_0. Following the similar argument for the right-eigenvectors, we can show that they are given by the solutions of the following,

$$\boldsymbol{w}_0(t)^\dagger(S^{t+1} + bS^{t+2}) = 0, \tag{3.14}$$

$$\sum_{j=1}^{n} w_{0j}(t) = 0, \quad t = 1, 2, \ldots, T. \tag{3.15}$$

The general form of the left-eigenvector $\boldsymbol{w}_0(t)$ is hence given by

$$\boldsymbol{w}_0(t) = \left(\underbrace{0, \cdots, 0}_{n-(t+1)}, w_{0,n-t}(t), \ldots, w_{0,n}(t) \right)^\mathsf{T} \tag{3.16}$$

with the condition (3.15). For a given set of generalized right-eigenvectors $\{\boldsymbol{v}_0^{(\ell,q)}(t) : \ell = 1, 2, \ldots, t, q = 1, \ldots, d_0^{(\ell)}(t)\}$, first we determine the left-eigenvectors (3.16) with (3.15), which we write as $\boldsymbol{w}_0^{(\ell,d_0^{(\ell)}(t))}(t)$, $\ell = 1, 2, \ldots, t$ by convention, so that they satisfy the *bi-orthonormality relation*,

$$\langle \boldsymbol{w}_0^{(\ell,d_0^{(\ell)}(t))}(t), \boldsymbol{v}_0^{(r,q)}(t) \rangle = \delta_{\ell,r}\delta_{d_0^{(\ell)}(t),q}, \quad \ell, r = 1, 2, \ldots, t, \quad q = 1, 2, \ldots, d_0^{(\ell)}(t). \tag{3.17}$$

As shown above for the generalized right-eigenvectors, we can also prove the following for $t = 1, 2, \ldots, T-1$. For each left-eigenvector $\boldsymbol{w}_0^{(\ell,d_0^{(\ell)}(t))}(t)$, $\ell = 1, 2, \ldots, t$, the generalized

16

left-eigenvectors, $\boldsymbol{w}_0^{(\ell, d_0^{(\ell)}(t)-q)}(t)$, $q = 1, 2, \ldots, d_0^{(\ell)}(t) - 1$, are given by the solutions of the following Jordan chain,

$$\boldsymbol{w}_0^{(\ell, d_0^{(\ell)}(t)-q)}(t)^\dagger (S^{t+1} + bS^{t+2}) = \boldsymbol{w}_0^{(\ell, d_0^{(\ell)}(t)-(q-1))}(t)^\dagger,$$

$$\sum_{j=1}^n w_{0j}^{(\ell, d_0^{(\ell)}(t)-q)}(t) = 0, \quad q = 1, 2, \ldots, d_0^{(\ell)}(t) - 1. \tag{3.18}$$

They are uniquely determined by the bi-orthonormality condition,

$$\langle \boldsymbol{w}_0^{(\ell, p)}(t), \boldsymbol{v}_0^{(r, q)}(t) \rangle = \delta_{\ell r} \delta_{p, q}, \quad \ell, r = 1, 2, \ldots, t, \quad p, q = 1, \ldots, d_0^{(\ell)}(t). \tag{3.19}$$

Remark 3.3 *Although the right-eigenvalues $\boldsymbol{v}_0^{(\ell, 1)}(t)$, $\ell = 1, 2, \ldots, t$ are simple as shown by (3.4), explicit expressions for the generalized right-eigenvectors $\boldsymbol{v}_0^{(\ell, q)}(t)$, $q = 2, 3, \ldots, d_0^{(\ell)}(t)$ become more complicated. For an example, here we show the results for $n = 6$ at time $t = 2$. There are $t = 2$ right-eigenvectors in the simple form, $\boldsymbol{v}_0^{(1,1)} = (1, -1, 0, 0, 0, 0)^\mathsf{T}$ and $\boldsymbol{v}_0^{(2,1)} = (1, 0, -1, 0, 0, 0)^\mathsf{T}$. Since $d_0^{(1)}(2) = d_0^{(2)}(2) = \lfloor 6/(2+1) \rfloor = 2$, we have one generalized right-eigenvector for each as*

$$\boldsymbol{v}_0^{(1,2)}(2) = (-b, 0, 0, 1 + b, -1, 0)^\mathsf{T}, \quad \boldsymbol{v}_0^{(2,2)}(2) = (-b + b^2, 0, 0, 1 - b^2, b, -1)^\mathsf{T},$$

respectively. Here we have followed the choice (3.13). The generalized left-eigenvectors are then determined uniquely by solving the Jordan chain (3.18) with the orthonormality condition (3.19) as

$$\boldsymbol{w}_0^{(1,1)}(2) = \left(\frac{1+b}{3+2b}, -\frac{2+b}{3+2b}, \frac{1+b}{3+2b}, \frac{b(1+2b)}{(3+2b)^2}, -\frac{2b(1+b)}{(3+2b)^2}, -\frac{2b(1+b)}{(3+2b)^2} \right)^\dagger,$$

$$\boldsymbol{w}_0^{(1,2)}(2) = \left(0, 0, 0, \frac{1+b}{3+2b}, -\frac{2-b^2}{3+2b}, \frac{1-b-b^2}{3+2b} \right)^\dagger,$$

$$\boldsymbol{w}_0^{(2,1)}(2) = \left(\frac{1}{3+2b}, \frac{1}{3+2b}, -\frac{2(1+b)}{3+2b}, \frac{4b}{(3+2b)^2}, \frac{b(1+2b)}{(3+2b)^2}, \frac{b(1+2b)}{(3+2b)^2} \right)^\dagger,$$

$$\boldsymbol{w}_0^{(2,2)}(2) = \left(0, 0, 0, \frac{1}{3+2b}, \frac{1+b}{3+2b}, -\frac{2+b}{3+2b} \right)^\dagger.$$

Remark 3.4 *At each time $t = 1, 2, \ldots, T - 1$, the first ($q = 2$) generalized right-eigenvector is given by*

$$\boldsymbol{v}_0^{(\ell,2)}(t)$$
$$= \left(\frac{b\{-1 + (-b)^\ell\}}{1+b}, \underbrace{0, \cdots, 0}_{t}, 1 - (-b)^\ell, -(-b)^{\ell-1}, \cdots, -(-b), -1, \underbrace{0, \cdots, 0}_{n-t-\ell-2} \right)^\mathsf{T}, \tag{3.20}$$

provided $n \geq (t+1) + (\ell+1)$, where the choice 3.13 was taken. The proof of (3.20) is given in a general setting in Appendix A. When $b = 0$, this is reduced to be the inverse shifts of

$\boldsymbol{v}_0^{(\ell,1)}(t)$ *given by* (3.4),

$$\begin{aligned}
\boldsymbol{v}_0^{(\ell,2)}(t) &= S^{\mathsf{T}} \boldsymbol{v}_0^{(\ell,1)}(t) \\
&= (\underbrace{0, \cdots, 0}_{t+1}, 1, \underbrace{0, \cdots, 0}_{\ell-1}, -1, \underbrace{0, \cdots, 0}_{n-t-\ell-2}).
\end{aligned}$$

Explicit expressions for the generalized right- and left-eigenvectors are given for the case $b = 0$ in Appendix B.

3.2 Jordan decomposition of resolvent and generalized condition numbers

For each time $t = 1, 2, \ldots, T$ and $\ell = 1, 2, \ldots, t$, define the $n \times d_0^{(\ell)}(t)$ rectangular matrices

$$V_{0,\ell}(t) := \left(\boldsymbol{v}_0^{(\ell,1)}(t)\, \boldsymbol{v}_0^{(\ell,2)}(t) \, \cdots \, \boldsymbol{v}_0^{(\ell,d_0^{(\ell)}(t))}(t) \right),$$

$$W_{0,\ell}(t) := \left(\boldsymbol{w}_0^{(\ell,1)}(t)\, \boldsymbol{w}_0^{(\ell,2)}(t) \, \cdots \, \boldsymbol{w}_0^{(\ell,d_0^{(\ell)}(t))}(t) \right).$$

Then, by the construction of the generalized eigenspaces given in Section 3.1, we have

$$S^{(b)}(t, \delta J) = \sum_{\ell=1}^{t} V_{0,\ell}(t) S_{d_0^{(\ell)}(t)} W_{0,\ell}(t)^{\dagger} + \sum_{j=1}^{p_1(t)+1} \lambda_j(t) P_j(t), \tag{3.21}$$

at each time $t = 1, 2, \ldots, T$, where we have defined the projection operators as

$$P_j(t) := \boldsymbol{v}_j(t) \boldsymbol{w}_j(t)^{\dagger} \in \mathbb{C}^{n \times n}, \quad j = 1, 2, \ldots, p_1(t)+1. \tag{3.22}$$

Remark 3.5 *For each time $t = 1, 2, \ldots, T$, define the $n \times n$ matrices*

$$V(t) := \left(V_{0,1}(t)\, V_{0,2}(t) \, \cdots V_{0,t}(t)\, \boldsymbol{v}_1(t)\, \boldsymbol{v}_2(t) \cdots \, \boldsymbol{v}_{p_1(t)+1} \right),$$

$$W(t) := \left(W_{0,1}(t)\, W_{0,2}(t) \, \cdots W_{0,t}(t)\, \boldsymbol{w}_1(t)\, \boldsymbol{w}_2(t) \cdots \, \boldsymbol{w}_{p_1(t)+1} \right).$$

Then

$$W(t) = V(t)^{-1}, \tag{3.23}$$

and

$$W(t) S^{(b)}(t, \delta J) V(t) = \mathbb{J}(t) \oplus \operatorname{diag}\left(\lambda_1(t), \lambda_2(t), \cdots, \lambda_{p_1(t)+1}(t) \right), \quad t = 1, 2, \ldots, T,$$

where

$$\mathbb{J}(t) = \bigoplus_{\ell=1}^{t} S_{d_0^{(\ell)}(t)}.$$

In order to calculate $W(t)$ by (3.23)*, we need to know the exact values of non-zero eigenvalues $\lambda_j(t)$ and their eigenvectors $\boldsymbol{v}_j(t)$, $j = 1, 2, \ldots, p_1(t)+1$. The method using bi-orthonormality relations explained in Section 3.1 gives the parts of $W(t)$ associated with λ_0; $W_{0,\ell}(t)$, $\ell = 1, 2, \ldots, t$, without these information.*

Let I be the $n \times n$ identity matrix. The *resolvents* of $(S^{(b)}(t, \delta J))_{1 \le t \le T}$ are then expanded as

$$\left(zI - S^{(b)}(t, \delta J)\right)^{-1} = \sum_{\ell=1}^{t} V_{0,\ell}(t) \left(zI - S_{d_0^{(\ell)}(t)}\right)^{-1} W_{0,\ell}(t)^\dagger + \sum_{j=1}^{p_1(t)+1} \frac{1}{z - \lambda_j(t)} P_j(t)$$

$$= \sum_{\ell=1}^{t} V_{0,\ell}(t) \left(\frac{1}{z}I + \frac{1}{z^2} S_{d_0^{(\ell)}(t)} + \cdots + \frac{1}{z^{d_0^{(\ell)}(t)}} S_{d_0^{(\ell)}(t)}^{d_0^{(\ell)}(t)-1}\right) W_{0,\ell}(t)^\dagger$$

$$+ \sum_{j=1}^{p_1(t)+1} \frac{1}{z - \lambda_j(t)} P_j(t), \quad t = 1, 2, \ldots, T, \tag{3.24}$$

This formula is a special case of Eq.(5.23) on page 40 in [19]. For each $\ell \in \{1, 2, \ldots, t\}$, $S_{d_0^{(\ell)}(t)}^{d_0^{(\ell)}(t)-q} \in \mathbb{C}^{d_0^{(\ell)}(t) \times d_0^{(\ell)}(t)}$ with $q \in \{1, 2, \ldots, d_0^{(\ell)}(t)\}$ is a matrix whose (j, k)-entries are 1 if $k - j = d_0^{(\ell)}(t) - q$, and are zero otherwise. Hence (3.24) is written as

$$\left(zI - S^{(b)}(t, \delta J)\right)^{-1}$$

$$= \sum_{\ell=1}^{t} \sum_{q=1}^{d_0^{(\ell)}(t)} \frac{1}{z^{d_0^{(\ell)}(t)-q+1}} \left(v_0^{(\ell,1)}(t) \, v_0^{(\ell,2)}(t) \, \cdots \, v_0^{(\ell,q)}(t)\right) \begin{pmatrix} w_0^{(\ell,d_0^{(\ell)}(t)-q+1)}(t)^\dagger \\ w_0^{(\ell,d_0^{(\ell)}(t)-q+2)}(t)^\dagger \\ \cdots \\ w_0^{(\ell,d_0^{(\ell)}(t))}(t)^\dagger \end{pmatrix}$$

$$+ \sum_{j=1}^{p_1(t)+1} \frac{1}{z - \lambda_j(t)} P_j(t), \quad t = 1, 2, \ldots, T. \tag{3.25}$$

For a matrix $M \in \mathbb{C}^{n \times n}$, the 2-norm of M is defined by

$$\|M\| := \max_{x \in \mathbb{C}^n} \frac{\|Mx\|}{\|x\|} = \max_{x \in \mathbb{C}^n : \|x\|=1} \|Mx\|,$$

where $\|x\|$ denotes the 2-norm of vector x. Therefore, for $t = 1, 2, \ldots, T$, as $z \to \lambda_j(t)$, $j = 1, 2, \ldots, p_1(t) + 1$,

$$\|(zI - S^{(b)}(t, \delta J))^{-1}\| = |z - \lambda_j(t)|^{-1} \|P_j(t)\| + O(1)$$

and as $z \to 0$,

$$\|(zI - S^{(b)}(t, \delta J))^{-1}\| \le |z|^{-k_0(t)} \sum_{\ell : d_0^{(\ell)}(t) = k_0(t)} \|v_0^{(\ell,1)}(t) w_0^{(\ell,d_0^{(\ell)}(t))}(t)^\dagger\| + O(|z|^{-k_0(t)+1}).$$

We see that

$$\|P_j(t)\| = \|v_j(t) w_j(t)^\dagger\| = \|v_j(t)\| \|w_j(t)\| =: \kappa_j(t),$$

where the value $\kappa_j(t)$ is know as the *eigenvalue condition number* of $\lambda_j(t)$, $j = 1, 2, \cdots, T$ [26]. We also see that

$$\|\boldsymbol{v}_0^{(\ell,1)}(t)\boldsymbol{w}_0^{(\ell,d_0^{(\ell)}(t))}(t)^\dagger\| = \|\boldsymbol{v}_0^{(\ell,1)}(t)\|\|\boldsymbol{w}_0^{(\ell,d_0^{(\ell)}(t))}(t)\| =: \kappa_0^{(\ell)}(t), \tag{3.26}$$

which we may call the *generalized condition number* of λ_0 associated with its ℓ-th Jordan block such that $d_0^{(\ell)}(t) = k_0(t)$. We put

$$\kappa_0(t) := \max_{\ell:d_0^{(\ell)}(t)=k_0(t)} \kappa_0^{(\ell)}(t).$$

By Proposition 3.2, if $(t+1) \mid n$, $k_0(t) = \lfloor n/(t+1) \rfloor$ while if $(t+1) \nmid n$, $k_0(t) = \lfloor n/(t+1) \rfloor + 1$. Hence

$$k_0(t) \leq \frac{n+t+1}{t+1}.$$

Moreover, Proposition 3.2 gives that, if $(t + 1) \mid n$,

$$\sharp\{\ell : d_0^{(\ell)}(t) = k_0(t)\} = \sharp\{\ell : 1 \leq \ell \leq t\} = t,$$

and if $(t + 1) \nmid n$,

$$\sharp\{\ell : d_0^{(\ell)}(t) = k_0(t)\} = \sharp\{\ell : 1 \leq \ell \leq n - (t+1)\lfloor n/(t+1) \rfloor - 1\} \leq t.$$

Then we have obtained the following estimates. See [26, Section 52].

Proposition 3.6 *For each time $t = 1, 2, \ldots, T$, there exist constants $r_j(t) > 0$ and $C_j(t) > 0$, $j = 0, 1, \ldots, p_1(t) + 1$ such that*

$$\|(zI - S^{(b)}(t, \delta J))^{-1}\| \leq C_0(t)|z|^{-(n+t+1)/(t+1)} \tag{3.27}$$

for all z satisfying $|z| \leq r_0(t)$, and

$$\|(zI - S^{(b)}(t, \delta J))^{-1}\| \leq C_j(t)|z - \lambda_j(t)|^{-1} \tag{3.28}$$

for all z satisfying $|z - \lambda_j(t)| \leq r_j(t)$, $j = 1, 2, \ldots, p_1(t) + 1$. The infimum of possible value for $C_0(t)$ is $t\kappa_0(t)$, and those for $C_j(t)$ are $\kappa_j(t)$, $j = 1, 2, \ldots, p_1(t) + 1$.

3.3 Time-dependent pseudospectra

The singularities of resolvent are exactly eigenvalues of the matrix. In (3.24), the non-zero eigenvalues $\lambda_j(t), j = 1, 2, \ldots, p_1 + 1$ give simple poles of the resolvent. The singularity at the zero-eigenvalue λ_0 is realized as the superpositions of poles with orders from 1 to $d_0^{(\ell)}(t)$ for $\ell = 1, 2, \ldots, t$ due to the Jordan-block structure of the generalized eigenspace associated with λ_0. This fact implies that the 2-norm of resolvent takes large values even at the places in $\mathbb{C}$ far from λ_0. The set of the points on $\mathbb{C}$ which are not necessarily eigenvalues exactly but at which the 2-norm of resolvent becomes large is called the *pseudospectrum*.

Definition 3.7 ([23, 26]) *Let $M \in \mathbb{C}^{n \times n}$ and $\varepsilon > 0$ be arbitrary. The ε-pseudospectrum $\sigma_\varepsilon(M)$ of M is the set of $z \in \mathbb{C}$ such that*

$$\|(zI - M)^{-1}\| > \varepsilon^{-1}. \tag{3.29}$$

Hence, the comparison of Proposition 3.6 with Definition 3.7 gives the following. For $\zeta \in \mathbb{C}$ and $r > 0$, let $\mathbb{D}(\zeta, r) := \{z \in \mathbb{C} : |z - \zeta| < r\}$.

Theorem 3.8 *Let $0 < \varepsilon < 1$. For each time $t = 1, 2, \ldots, T$, there exist constants $C_j(t) > 0$, $j = 0, 1, \ldots, p_1(t) + 1$ such that*

$$\sigma_\varepsilon(S^{(b)}(t, \delta J)) \subseteq \mathbb{D}\left(0, (\varepsilon C_0(t))^{(t+1)/(n+t+1)}\right) \bigcup_{j=1}^{p_1(t)+1} \mathbb{D}\left(\lambda_j(t), \varepsilon C_j(t)\right). \tag{3.30}$$

The infimum of possible value for $C_0(t)$ is $t\kappa_0(t)$, and those for $C_j(t)$ are $\kappa_j(t)$, $j = 1, 2, \ldots, p_1(t) + 1$.

Remark 3.9 (i) *With fixed n and t, as $\varepsilon \to 0$, the ε-pseudospectrum including λ_0 shrinks to the origin. For large n, the exponent $(t+1)/(n+t+1)$ becomes small positive value. Hence, the pseudospectrum including λ_0 should become a singleton $\{\lambda_0\}$ in the limit $\varepsilon \to 0$, as a matter of course, but the size reduction of the pseudospectrum will be very slow for large n.*

(ii) *With fixed n, as time t increases from 1 to T, $(t+1)/(n+t+1)$ increases monotonically from $2/(n+2)$ to $(n-1)/(2n-1) \simeq 1/2$. This suggests that, if $\varepsilon < \{\max_{t:1 \leq t \leq T} t\kappa_0(t)\}^{-1}$, the ε-pseudospectrum including λ_0 shrinks as time t is increasing. Notice that as given by (B.2), when $b = 0$,*

$$\left\{\max_{t:1 \leq t \leq T} t\kappa_0(t)\right\}^{-1} = \{t\kappa_0(t)|_{t=T}\}^{-1} = \{2(n-2)(n-1)\}^{-1/2}.$$

This behaves as $n^{-1}/\sqrt{2}$ as $n \to \infty$. The size reduction of the ε-pseudospectrum including λ_0 in time shows the relaxation of defectivity of λ_0.

(iii) *On the other hand, with fixed time t, as the size of matrix n increases, $(t+1)/(n+t+1) \searrow 0$. This implies that for a given $\varepsilon \in (0,1)$, the ε-pseudospectrum including λ_0 expands as $n \to \infty$.*

4 Numerical Analysis

## 4.1 Sensitivity of defective eigenvalue to perturbations

For a matrix M, its spectrum (the set of eigenvalues) is denoted by $\sigma(M)$. It is proved that Definition 3.7 of pseudospectra given in Section 3.3 is equivalent with the following definition [23] [26, Theorem 2.1].

Definition 4.1 *The ε-pseudospectrum of a matrix $M \in \mathbb{C}^{n \times n}$ with $\varepsilon > 0$ is the set of $z \in \mathbb{C}$ such that*

$$z \in \sigma(M + E)$$

for some matrix $E \in \mathbb{C}^{n \times n}$ with $\|E\| < \varepsilon$.

That is, for a given matrix, the ε-pseudospectrum is *not* the exact spectrum of the matrix, but it is the set of exact eigenvalues of some perturbed matrix $M + E$ with $\|E\| < \varepsilon$.

(a) $\widetilde{\delta} = 10^{-2}$ **(b)** $\widetilde{\delta} = 10^{-4}$ **(c)** $\widetilde{\delta} = 10^{-10}$
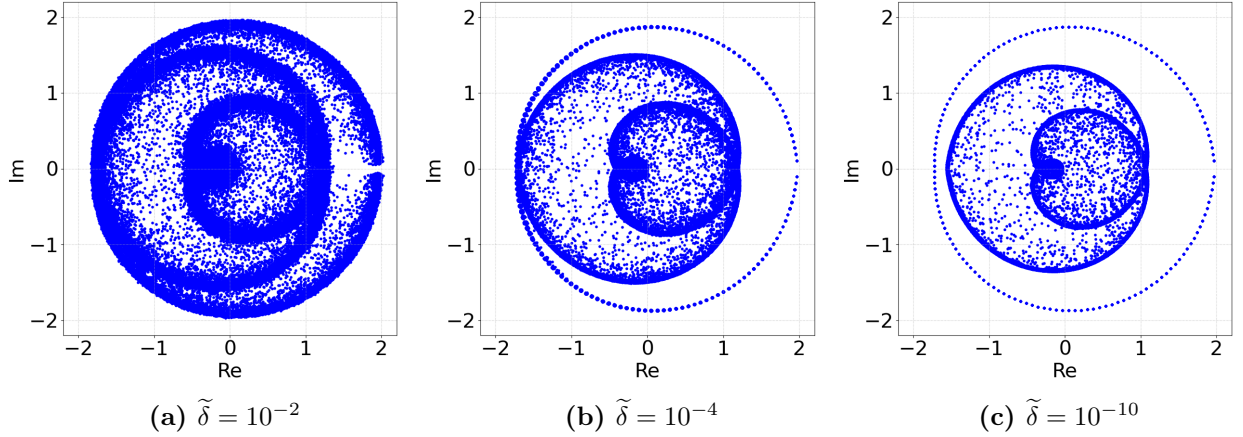
Figure 4: Numerically obtained eigenvalues are superposed for 200 i.i.d Gaussian random perturbations Z added to $S^{(b)}(t, \delta J)$ as (4.1) with each value of $\widetilde{\delta}$, where $n = 500$, $t = 2$, $b = 1$, and $\delta = 10^{-2}$. The outlier eigenvalue $\lambda_1(t)$ is not drawn in each figure, since it is located outside the frame.

Here we add Gaussian random perturbations to our dynamical systems (1.9) as

$$S^{(b)}(t, \delta J) + \widetilde{\delta} Z = S^{t+1} + bS^{t+2} + \delta J + \widetilde{\delta} Z, \tag{4.1}$$

where the entries of $Z = (Z_{jk})_{1 \leq j,k \leq n}$ are given by (1.5) and $\widetilde{\delta} \in \mathbb{C}$. Figure 4 shows the plots of numerically obtained eigenvalues for $n = 500$, $t = 2$, $b = 1$, and $\delta = 10^{-2}$. Each of Figs. 4a–4c shows the superpositions of the numerically obtained eigenvalues for 200 i.i.d. Z. The following are observed.

(i) Fig.4a shows the numerical result when $\widetilde{\delta}$ is equal to $\delta = 10^{-2}$. The obtained plots are similar to Fig.1b of the superpositions of 50 samples of numerically obtained eigenvalues for (1.6) with $n = 5000$, $m = t + 1 = 3$, $b = 1$, and $\widetilde{\delta} = 1/\sqrt{2n} = 10^{-2}$, although in (1.6) the all-ones matrix J was not added; in other words, $\delta = 0$. This suggests that, if $\delta = \widetilde{\delta}$, both of δJ and $\widetilde{\delta} Z$ are acting as perturbations to $S^{t+1} + bS^{t+2}$ and hence the eigenvalues of the perturbed system (4.1) tend to trace out the symbol curve of the Toeplitz operator $\widehat{S}^{t+1} + b\widehat{S}^{t+2}$, $b = 1$. See Fig.1c for the symbol curve [6, 26] for $m = t + 1 = 3$ and $b = 1$.

22

(ii)   As shown by Fig.4b, if $\widetilde{\delta}$ is set to be much smaller than δ, then the situation is realized such that the system $S^{(b)}(t, \delta J)$ including the term δJ is perturbed by Z. Now the outmost curve represents the $p_1(t)$ non-zero exact eigenvalues of the unperturbed system solving (2.8) of Theorem 2.1, except the outlier eigenvalue $\lambda_1(t)$ characterized by Proposition 2.3. (See Proposition 2.4 asserting a circular configurations of the non-zero exact eigenvalues of $S^{(b)}(t, \delta J)$ when n is sufficiently large.) Notice that $S^{(b)}(t, \delta J) = S^{t+1} + bS^{t+2} + \delta J$, $t = 1, 2, \ldots, T$ are still Toeplitz matrices, but they are neither *banded* nor in the Wiener class due to the all-ones matrix J. Hence we do not have any corresponding Toeplitz operators nor symbol curves. (For the relationship between the peudospectra of banded Toeplitz matrices and the exact spectra of corresponding Toeplitz operators, see [23], [26, Section 7].) When $\widetilde{\delta} = 10^{-10}$ as shown by Fig.4c, we observe separation of the symbol curve of $\widehat{S}^{t+1} + b\widehat{S}^{t+2}$ with $t = 2$ (see Fig.1c) into the outmost part and the inner part and the size of the latter is reduced. Such phenomena in pseudospectrum processes exhibiting *separation* of symbol curves and *dilatation* of their inner parts have not been reported in the previous studies on banded Toeplitz matrices with random perturbations [1, 2, 3, 4, 5, 24].

(iii)   The non-zero exact eigenvalues of the original $S^{(b)}(t, \delta J)$ are *insensitive* to random perturbation and the outmost part consisting of them keeps almost the same circular configuration. The inner part, in which the eigenvalues of perturbed system are densely distributed, expresses the pseudospectrum of including λ_0 of the original system. It continues to reduce its size as $\widetilde{\delta}$ decreases down to $\widetilde{\delta} = 10^{-30}$. Even if we put $\widetilde{\delta} = 0$, however, we observed the very similar result with the pattern for $\widetilde{\delta} = 10^{-30}$. This means that rounding errors in our personal computer will be $\simeq 10^{-30}$ and they also produce perturbations to $S^{(b)}(t, \delta J)$, and hence we can not realize $\widetilde{\delta} \to 0$ limit in the present numerical study. Such high *sensitivity of the defective eigenvalue λ_0* to very weak perturbations is consistent with the persistency of the ε-pseudospectrum including λ_0 as $\varepsilon \to 0$ mentioned in Remark 3.9 (i) in Section 3.3.
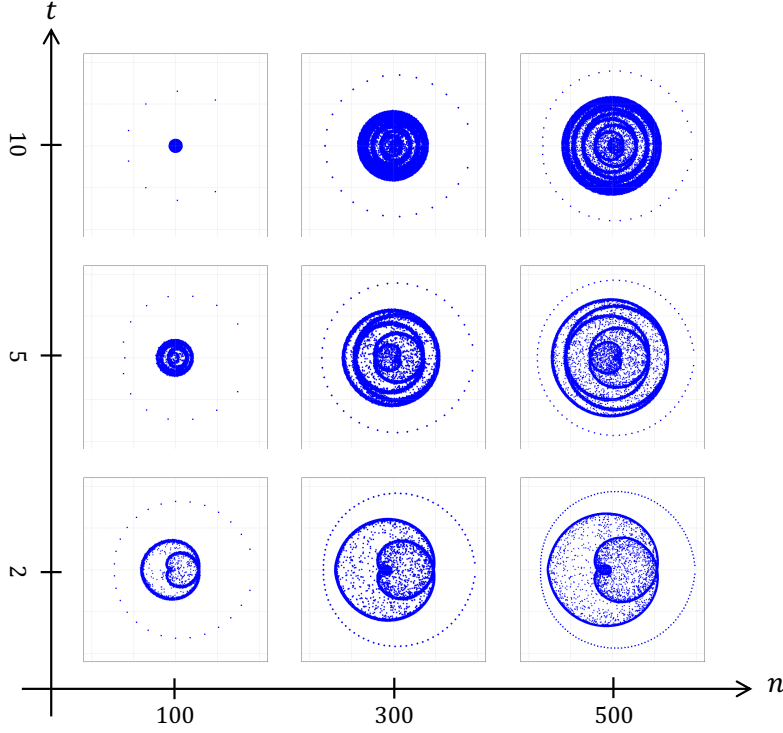
4.2 (t, n)-dependence of pseudospectra

Theorem 3.8 suggests that, with given b if we denote the linear size of the ε-pseudospectrum including λ_0 as R_ε for the present system $S^{(b)}(t, \delta J)$, it depends on ε, t, and n in the form

$$\log R_\varepsilon(t, n) \simeq c(\varepsilon, t, n)\frac{t + 1}{n + t + 1}, \quad t = 1, 2, \ldots, T := n - 2. \tag{4.2}$$

Here the coefficient c depends mainly on ε and its dependence on t and n will be small only though their logarithms. As mentioned by Remark 3.9, with a fixed $0 < \varepsilon \ll 1$, $R_\varepsilon(t, n)$ will decrease with increment of t and will expand with increment of n.

Figure 5 shows plots of the numerically obtained eigenvalues superposed for 200 i.i.d. Gaussian perturbed systems (4.1) with $b = 1$, $\delta = 10^{-2}$, and $\widetilde{\delta} = 10^{-10}$. Here, we set $n = 100, 200, 500$ and $t = 2, 5, 10$. In each figure, the non-zero exact eigenvalues $\lambda_j(t)$, $j = 2, 3, \cdots, p_1(t) + 1$ make the outmost circular configuration. Here $p_1(t) = \lfloor (n - 1)/(t + 1)$

Figure 5: Numerically obtained eigenvalues are superposed for 200 i.i.d Gaussian random perturbations Z added to $S^{(b)}(t, \delta J)$ as (4.1) with $b = 1$, $\delta = 10^{-2}$, and $\widetilde{\delta} = 10^{-10}$. Dependence on n and t is shown. The pseudospectrum including λ_0 is observed as an inner domain fulfilled by dots. It shrinks with increment of t showing the relaxation process of the defectivity of λ_0 for each n. On the other hand, as n increases the inner part shows expansion. The curves lined up by the eigenvalues of perturbed systems seem to draw the inner parts of symbol curves of $\widehat{S}^{t+1} + b\widehat{S}^{t+2}$.

1)⌋, and the radius of the circle increases (resp. decreases) as n (resp. t) increases. The pseudospectrum including λ_0 is observed as an inner disk fulfilled by dots, which indeed shrinks with increment of t and expands with increment of n, keeping separation from the outmost circle of exact eigenvalues. Notice that as t increases more complicated structures appear in the inner disk. They reflect the inner parts of the symbol curves of $\widehat{S}^{t+1} + b\widehat{S}^{t+2}$ which become more complicated as t increases [21].

Given b, we performed numerical calculation of eigenvalues of the randomly perturbed system (4.1) with $\delta = 10^{-2}$ and $\widetilde{\delta} = 10^{-10}$ for a variety of t and n. For each numerical result, which is represented by the similar figure to Fig.4c, we eliminated the plots of non-zero eigenvalues $\lambda_j(t)$, $j = 1, 2, \ldots, p_1(t) + 1$ making the outmost circle. We write the remaining eigenvalues as $\widetilde{\lambda}_j(t)$, $j = 1, 2, \ldots, m$, where m is the total number of them. Then
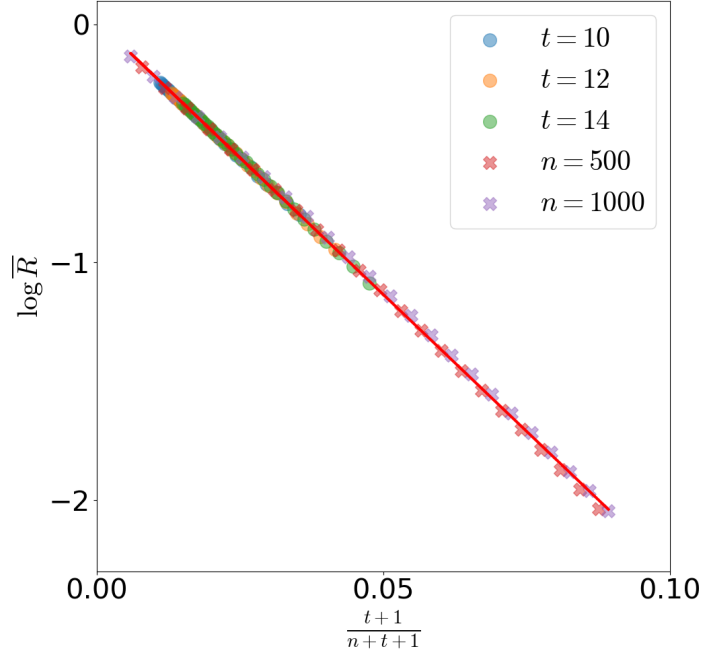
Figure 6: Numerically evaluated radius $\overline{R}(t,n)$ defined by (4.3) are plotted for the perturbed system (4.1) with $b = 0$, $\delta = 10^{-2}$, and $\widetilde{\delta} = 10^{-10}$ for a variety of values of t and n. The results are superposed for $t = 8, 10, 12$ with increasing n by 20 from 120 to 980, for $n = 500$ with increasing t by 2 from 2 to 48, and for $n = 1000$ with increasing t by 4 from 2 to 98, respectively. The linear fitting (4.4) of all these data is shown by the red line, which gives $c_1 \simeq -23$ and $c_2 \simeq 0.02$.

we numerically evaluated the mean radius $\overline{R}(t,n)$ of them,

$$\overline{R}(t,n) := \frac{1}{m} \sum_{j=1}^{m} |\widetilde{\lambda}_j(t)|. \tag{4.3}$$

We have observed that, when $b = 0$ (resp. $b = 1$), $\overline{R}(t,n)$ is approximately equal to (resp. 2/3 of) the radius of the boundary of the region where $\widetilde{\lambda}_n(t)$ are distributed. Figure 6 shows $\log \overline{R}(t,n)$ versus $(t+1)/(n+t+1)$ in the simple case with $b = 0$. The linear fitting

$$\log \overline{R}(t,n) = c_1 \frac{t+1}{n+t+1} + c_2 \tag{4.4}$$

works well with $c_1 \simeq -23$ and $c_2 \simeq 0.02$. It is expected that c_1 is approximately equal to $\log \varepsilon$. Then the above fitting will give $\varepsilon = e^{-23} \simeq 1.0 \times 10^{-10}$. This is consistent with the choice of the coefficient $\widetilde{\delta} = 10^{-10}$ in the numerical simulation of (4.1). Hence, although the formula (4.2) is an approximation, it seems to be valid. We notice that Theorem 3.8 with Remark 3.9 and Fig.6 supports Conjecture 5.5 given in [21].

5 Future Problems

We list out future problems.

(1) For $n \geq 2$, let h be a polynomial of $\deg h \geq 1$, that is,

$$h(s) = h(s, \{b_j\}_{j \geq 1}) := \sum_{j=1}^{n-1} b_j s^j \tag{5.1}$$

with $b_j \in \mathbb{C}$, $j = 1, 2, \ldots, n-1$. We consider a nilpotent Toeplitz matrix

$$S_n(t, \{b_j\}_{j \geq 1}) := S_n^{t+1}(I + h(S_n, \{b_j\}_{j \geq 1})), \quad t = 1, 2, \ldots, T := n - 2, \tag{5.2}$$

where S_n is the shift matrix (1.1) of size n and $b_j \in \mathbb{C}$, $j \geq 1$. At each time $t \geq 1$, we consider a one parameter (the matrix size $n = 2, 3, \ldots$) family, $\{S_n(t, \{b_j\}_{j \geq 1})\}_{n \geq 2}$. If the Toeplitz matrices are banded; that is, $b_j = 0$ for $j \geq {}^\exists w$ or in the Wiener class; $\sum_{j \geq 1} |b_j| < \infty$, the symbol is defined by

$$f(z) = f(z, t, \{b_j\}_{j \geq 1}) := z^{t+1}(1 + h(z)). \tag{5.3}$$

For a given point $z \in \mathbb{C} \setminus f(\mathbb{T})$, $w(f, z)$ is defined to be the *winding number* of the curve $f := f(\mathbb{T})$ about z in the usual positive (counterclockwise) sense. The following is proved [23, 26].

(i) Consider the triangular Toeplitz operator corresponding to (5.2)

$$\widehat{S}(t, \{b_j\}_{j \geq 1}) := \widehat{S}^{t+1}(\widehat{I} + h(\widehat{S}, \{b_j\}_{j \geq 1})),$$

where $\widehat{I}$ is the identity operator. Then its spectrum is given by

$$\sigma(\widehat{S}(t, \{b_j\}_{j \geq 1})) = f(\mathbb{T}) \cup \{z \in \mathbb{C} : w(f, z) \neq 0\}; \tag{5.4}$$

that is, the symbol curve together with all the points enclosed by the symbol curve with nonzero winding numbers.

(ii) At any point $z \in \sigma(\widehat{S}(t, \{b_j\}_{j \geq 1}))$, for some $C > 1$ and for all sufficiently large n,

$$\|(zI - S_n(t, \{b_j\}_{j \geq 1})^{-1}\| \geq C^n. \tag{5.5}$$

Comparing this fact with Definitions 3.7 and 4.1, we can conclude that if we add dense random perturbations to $S_n(t, \{b_j\}_{j \geq 1})$ at each time $t = 1, 2, \ldots, T$, the eigenvalues tends to fill the spectra $\sigma(\widehat{S}(t, \{b_j\}_{j \geq 1}))$. Moreover, if we plot the numerically obtained eigenvalues for the perturbed system, the symbol curve $f(\mathbb{T})$ seems to be lined up by the dots, as demonstrated by Fig.1. In this sense, the pseudospectra of $S_n(t, \{b_j\}_{j \geq 1})$, $n \geq 2$, $t = 1, 2, \ldots, T$ are well characterized by the spectra of the corresponding triangular Toeplitz operators $\widehat{S}(t, \{b_j\}_{j \geq 1})$, $t = 1, 2, \ldots, T$ and their symbol curves.

On the other hand, our matrix $S_n^{(b)}(t, \delta J)$, for $n \geq 2$, $t = 1, 2, \ldots, T$ given by (1.9) is not banded due to addition of the all-ones matrix J. Hence there is no corresponding Toeplitz operator nor symbol curve. Nevertheless, we have observed the phenomenon such that if we add the complex random Gaussian matrices as perturbations, the numerically obtained eigenvalues are lined up along some curves and they tend to fill only inside of the domains where that curve exists. As demonstrated by Figs.4 and 5, these curves seem to be the *inner parts* of the symbol curve $f(\mathbb{T})$ of $\widehat{S}^{t+1} + b\widehat{S}^{t+2}$, which is obtained by eliminating the outmost closed simple curve and is composed of $t - 1$ smaller closed simple curves osculating each other. (See also Section 4.2 in [21].) The outmost closed simple curve consists of the non-zero eigenvalues of the unperturbed matrix and they are insensitive to perturbations. As shown by Figs.4 and 5, the inner parts are shrinking in time and hence the gaps between the outmost curve consisting of the original eigenvalues and the inner part fulfilled by eigenvalues of perturbed systems become larger as time t is passing. Such phenomena showing separation of symbol curves and size-reduction of their inner parts have not been reported in the previous studies of *banded* Toeplitz matrices with random perturbations (see [1, 2, 3, 4, 5, 24] and references therein). The present new phenomena found in the pseudospectrum processes express the relaxation processes of the defective eigenvalue λ_0. Mathematical understanding of such separation and dilatation of symbol curves will be a challenging future problem.

(a) $b_1 = 2, b_j = 0 \, (j \geq 2)$ **(b)** $b_1 = b_2 = 1, b_j = 0 \, (j \geq 3)$ **(c)** $b_1 = 2, b_2 = 3, b_j = 0 \, (j \geq 3)$
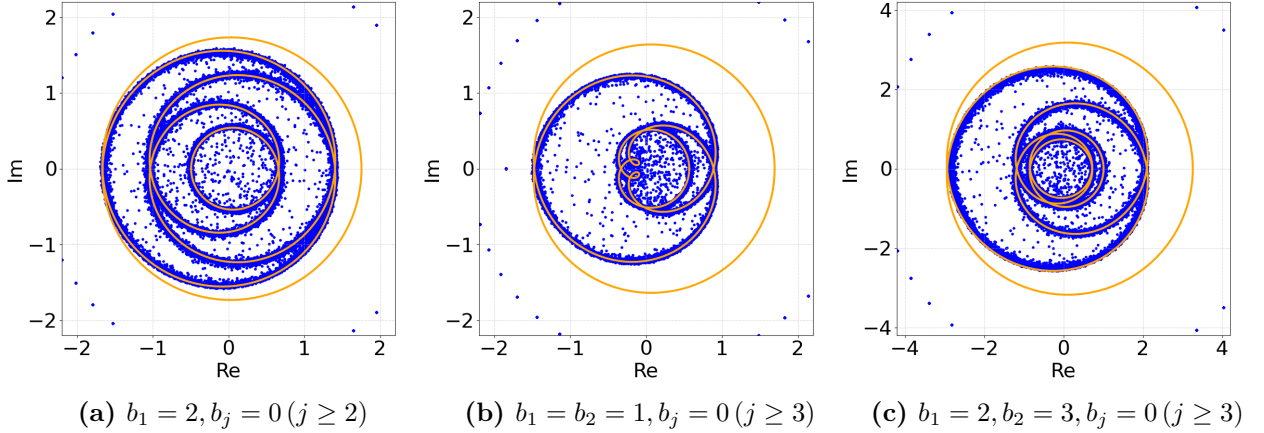
Figure 7: Numerically obtained eigenvalues are superposed for 200 i.i.d Gaussian random perturbations Z added to $S_n(t, \{b_j\}_{j \geq 1}) + \delta J$ as (5.9) with the specified choices of $\{b_j\}_{j \geq 1}$, where $n = 200$, $t = 3$, $\delta = 10^{-2}$, and $\varepsilon = 10^{-10}$. The symbol curves with size reduction (5.6) are drawn by red curves. In the present cases, $\varpi = (3 + 1) \times \{200/(3 + 1)\} = 200$ and hence $\varepsilon^{1/\varpi} = (10^{-10})^{1/200} = 10^{-1/20} = 0.891 \cdots$.

Based on numerical study, we propose a conjecture as explained below. We put

$$\varpi = \varpi(t, n) := (t + 1)k_0(t), \quad t = 1, 2, \ldots, T,$$

where $k_0(t)$ is the index of λ_0 given by (1.13). Assume that $\varepsilon > 0$ is small enough so that the ε-pseudospectra are separated without any intersection into one ε-pseudospectrum including λ_0, which is denoted by σ_ε^0, and other parts including $\lambda_j(t)$, $j = 1, 2, \ldots,$ $p_1(t) + 1$. Consider the symbol curve with size reduction

$$f_\varepsilon := \{f(re^{i\theta}) : r = \varepsilon^{1/\varpi}, \theta \in [0, 2\pi)\}, \tag{5.6}$$

where f is given by (5.3). Let $\mathcal{I} = \mathcal{I}(t, \{b_j\}_{j\geq 1}) \subset [0, 2\pi)$ be the interval of the argument θ such that $\{f(\varepsilon^{1/\varpi}e^{i\theta}) : \theta \in \mathcal{I}\}$ provides the outmost closed simple curve of f_ε. That is, if we define $\theta_0 := \min\{\theta \in (0, 2\pi) : \mathrm{Im} f(\varepsilon^{1/\varpi}e^{i\theta}) = 0\}$, (i.e., the smallest positive θ such that the curve (5.6) intersects with the real axis), then $\mathcal{I} = [0, \theta_0) \cup [2\pi - \theta_0, 2\pi)$. We conjecture that

$$\sigma_\varepsilon^0(S_n(t, \{b_j\}_{j\geq 1}) + \delta J) = \widetilde{f}_\varepsilon \cup \{z \in \mathbb{C} : w(\widetilde{f}_\varepsilon, z) \neq 0\}, \tag{5.7}$$

where

$$\widetilde{f}_\varepsilon := \{f(re^{i\theta}) : r = \varepsilon^{1/\varpi}, \theta \in [0, 2\pi) \setminus \mathcal{I}\}, \tag{5.8}$$

and $w(\widetilde{f}_\varepsilon, z)$ denotes the winding number of the curve $\widetilde{f}_\varepsilon$ about z. Notice that (5.7) does not depend on δ. We have numerically studied the randomly perturbed systems,

$$S_n(t, \{b_j\}_{j\geq 1}) + \delta J + \varepsilon Z, \quad t = 1, 2, \ldots, T, \tag{5.9}$$

where $Z = (Z_{jk})_{1\leq j,k}$ is the Gaussian random matrix with the entries (1.5) and $0 < \varepsilon \ll \delta \ll 1$. Figure 7 shows three examples of the superpositions of numerically obtained eigenvalues. There the symbol curves with size reduction (5.6) are also drawn by red curves. The eigenvalues of the randomly perturbed systems tend to trace out the inner parts (5.8) of the size-reduced symbol curves (5.6). Independence of $\sigma_\varepsilon^0(S_n(t, \{b_j\}_{j\geq 1}) + \delta J)$ on δ has been numerically confirmed provided $\delta \gg \varepsilon$.

(2) We have established a procedure to determine the generalized eigenspace associated with λ_0 in Section 3.1 without using any information of the eigenspaces associated with the non-zero eigenvalues. The explicit expressions of the generalized eigenvectors for λ_0 are given in Appendix B in the case $b = 0$. Similar calculation is desired for the general case with $b \neq 0$.

For the systems (5.2), here we have reported our detail study in the special case with $b_1 = b \in \mathbb{C}$ and $b_j = 0$, $j \geq 2$. Generalization including b_j, $j \geq 2$ should be studied. See Appendix A.

Another direction of generalization of the present dynamics will be given by replacing the all-ones matrix J by a matrix in the form, $M = (\boldsymbol{m}\ c_2\boldsymbol{m}\ c_3\boldsymbol{m}\ \cdots\ c_n\boldsymbol{m})^\mathsf{T}$, where $\boldsymbol{m} \in V_n$ and $c_j \in \mathbb{C}$, $j = 2, 3, \ldots, n$. In this case, $M\boldsymbol{c} = \langle \boldsymbol{v}, \overline{\boldsymbol{m}}\rangle\boldsymbol{c}$ with $\boldsymbol{c} = (1, c_2, c_3, \ldots, c_n)^\mathsf{T}$ and hence $\mathbf{1}$ and $\alpha(\boldsymbol{v}(t)) = \langle \boldsymbol{v}(t), \mathbf{1}\rangle = \sum_{j=1}^n v_j(t)$ shall be replaced by $\boldsymbol{c}$ and $\langle \boldsymbol{v}(t), \overline{\boldsymbol{m}}\rangle$, respectively, in calculations. It will be possible to consider the discrete-time stochastic processes, in which the vectors $\boldsymbol{m}$ and $\boldsymbol{c}$ are randomly

28

distributed following some probability laws. (See [22] for the random nilpotent matrix model.)

We expect a meaningful connection between the present calculations of our dynamics of nilpotent Toeplitz matrices and the representation theory of the semisimple Lie groups via time-evolutionary Young diagrams [11, 16, 22] demonstrated by Fig.3.

(3) As mentioned in Section 1, one of the motivations of the present study is the observation by Burda et al.[9] of the non-Hermitian matrix-valued BM started from a nonnormal and defective matrix S. In the non-Hermitian matrix-valued stochastic processes, the coupling between the eigenvalue processes and the time evolution of the *eigenvector-overlap matrices* is essential [7, 8, 9, 12, 18]. The square roots of the diagonal elements of the eigenvector-overlap matrices are the condition numbers of eigenvalues. In (3.26) in Section 3.2, we introduced a notion of generalized condition numbers, which represent overlap between the left- and the right-eigenvectors in the same Jordan block associated with the defective eigenvalue λ_0. We hope that the present study of the deterministic processes will lead us further understanding of the coupling systems of eigenvalue processes and eigenvector-overlap processes in nonnormal matrix-valued stochastic processes.

A   Proof of (3.20) in a general setting

For the shift matrix $S = S_n$ given by (1.1), we consider the dynamics, $(S_n(t, \{b_j\}_{j\geq 1}))_{t=1}^T$, defined by (5.2) with (5.1). Note that there is a polynomial $\widehat{h}(s)$ of $\deg \widehat{h} \geq 1$ such that $(I + h(S))(I + \widehat{h}(S)) = I$, since S is nilpotent. Given $\boldsymbol{v}$, we consider the following problem,

$$\{(S^{t+1}(I + h(S)) + \delta J\}\boldsymbol{w} = \lambda\boldsymbol{w} + \boldsymbol{v}.$$

We focus on the case where $\lambda = \lambda_0 = 0$, i.e.,

$$\{(S^{t+1}(I + h(S)) + \delta J\}\boldsymbol{w} = \boldsymbol{v}. \tag{A.1}$$

By (2.4), this is equivalent to

$$S^{t+1}(I + h(S))\boldsymbol{w} = \boldsymbol{v} - \delta\alpha(\boldsymbol{w})\mathbf{1}. \tag{A.2}$$

Lemma A.1 *Suppose $\boldsymbol{v} = (v_1, v_2, \ldots, v_n)$ such that $v_j = 0$ for some $j \geq n - t$. Then,*

$$\boldsymbol{w} = -\alpha\big(S^{-(t+1)}(I + \widehat{h}(S))\boldsymbol{v}\big)\boldsymbol{e}_1 + S^{-(t+1)}(I + \widehat{h}(S))\boldsymbol{v} \tag{A.3}$$

is a solution to (A.1), where $S^{-(t+1)}$ is defined by (3.11).

Proof By comparing the j-th coordinate of both sides of (A.2), we see that $\alpha(\boldsymbol{w}) = 0$ in (A.2), which is equivalent to

$$S^{t+1}\boldsymbol{w} = (I + \widehat{h}(S))\boldsymbol{v}, \quad \alpha(\boldsymbol{w}) = 0. \tag{A.4}$$

Therefore, for any $\boldsymbol{u} \in V_{t+1}$,

$$\boldsymbol{w} = \boldsymbol{u} + S^{-(t+1)}(I + \widehat{h}(S))\boldsymbol{v} \tag{A.5}$$

is a solution to (A.2) whenever $\alpha(\boldsymbol{w}) = 0$. Since

$$\boldsymbol{u} = -\alpha\big(S^{-(t+1)}(I + \widehat{h}(S))\boldsymbol{v}\big)\boldsymbol{e}_1 \in V_1 \tag{A.6}$$

and $\alpha(\boldsymbol{w}) = 0$, we see that $\boldsymbol{w}$ given in (A.3) is a solution to (A.2). ∎

Corollary A.2 *Let $1 + \widehat{h}(s) = \sum_{k=0}^{n-1} b_k s^k$ with $b_0 = 1$. Then, for $t + 2 + \ell \leq n$,*

$$\boldsymbol{w} = \Big(\sum_{k=1}^{\ell} b_k\Big)\boldsymbol{e}_1 + (1 - b_\ell)\boldsymbol{e}_{t+2} - \sum_{p=1}^{\ell} b_{\ell-p}\boldsymbol{e}_{t+2+p}. \tag{A.7}$$

is a solution to (A.1) for $\boldsymbol{v} = \boldsymbol{v}^{(\ell,1)}(t) = \boldsymbol{e}_1 - \boldsymbol{e}_{\ell+1}$.

Proof We consider the case where $\boldsymbol{v} = \boldsymbol{e}_1 - \boldsymbol{e}_{\ell+1}$.

$$S^{-(t+1)}(I + \widehat{h}(S))\boldsymbol{v} = S^{-(t+1)}\Big(\boldsymbol{v} + \sum_{k=1}^{n-1} b_k S^k \boldsymbol{v}\Big)$$

$$= S^{-(t+1)}\boldsymbol{v} - S^{-(t+1)}\sum_{k=1}^{\ell} b_k S^k \boldsymbol{e}_{\ell+1}$$

$$= \boldsymbol{e}_{t+2} - \sum_{k=0}^{\ell} b_k \boldsymbol{e}_{t+2+\ell-k}$$

$$= (1 - b_\ell)\boldsymbol{e}_{t+2} - \sum_{p=1}^{\ell} b_{\ell-p}\boldsymbol{e}_{t+2+p}$$

for $t + 2 + \ell \leq n$. Then,

$$\alpha(S^{-(t+1)}(I + \widehat{h}(S))\boldsymbol{v}) = -\sum_{k=1}^{\ell} b_k.$$

From Lemma A.1, a solution $\boldsymbol{w}$ to (A.2) is given by (A.7). The proof is complete. ∎

Example A.3 *Suppose $h(s) = bs$. Then, $\widehat{h}(s) = \sum_{k=1}^{n-1}(-b)^k s^k$. For $t + 2 + \ell \le n$,*

$$\boldsymbol{w} = \left\{\sum_{k=1}^{\ell}(-b)^k\right\}\boldsymbol{e}_1 + \{1 - (-b)^\ell\}\boldsymbol{e}_{t+2} - \sum_{p=1}^{\ell}(-b)^{\ell-p}\boldsymbol{e}_{t+2+p}$$

$$= \frac{b\{-1 + (-b)^\ell\}}{1+b}\boldsymbol{e}_1 + \{1 - (-b)^\ell\}\boldsymbol{e}_{t+2} - \sum_{p=1}^{\ell}(-b)^{\ell-p}\boldsymbol{e}_{t+2+p}.$$

This proves (3.20).

B Explicit expressions of the generalized eigenvectors associated with $\lambda_0 = 0$ when $b = 0$

Here we consider the case $b = 0$. Remind Proposition 3.2.

(i) The generalized left-eigenvectors for $\lambda_0 = 0$ are given by

$$\boldsymbol{v}_0^{(\ell,q)}(t) = \Big(\underbrace{0,\cdots,0}_{(t+1)(q-1)}, 1, \underbrace{0,\cdots,0}_{\ell-1}, -1, \underbrace{0,\cdots,0}_{t-\ell+n-(t+1)q} \Big)^{\mathsf{T}}, \quad q = 1, 2, \ldots, d_0^{(\ell)}(t).$$

(ii) When $(t+1) \mid n$, the left eigenvectors are given by

$$\boldsymbol{w}_0^{(\ell,d_0^{(\ell)}(t))}(t) = \frac{1}{t+1}\Big(\underbrace{0,\cdots,0}_{n-t-1}, \underbrace{1,\cdots,1}_{\ell}, -t, \underbrace{1,\cdots,1}_{t-\ell} \Big)^{\mathsf{T}}, \quad \ell = 1, 2, \ldots, t.$$

The generalized left-eigenvectors are then given by

$$\boldsymbol{w}_0^{(\ell,d_0^{(\ell)}(t)-q)}(t) = \frac{1}{t+1}\Big(\underbrace{0,\cdots,0}_{n-(q+1)(t+1)}, \underbrace{1,\cdots,1}_{\ell}, -t, \underbrace{1,\cdots,1}_{t-\ell}, \underbrace{0,\cdots,0}_{q(t+1)} \Big)^{\mathsf{T}},$$

$\ell = 1, 2, \ldots, t$, $q = 1, \ldots, d_0^{(\ell)}(t) - 1$.

(iii) When $(t+1) \nmid n$, we put $\xi := n \pmod{t+1} \in \{1, 2, \ldots, t\}$. Then, the left-eigenvectors are determined as

$$\boldsymbol{w}_0^{(\ell,d_0^{(\ell)}(t))}(t) = \frac{1}{\xi}\Big(\underbrace{0,\cdots,0}_{n-\xi}, \underbrace{1,\cdots,1}_{\ell}, 1-\xi, \underbrace{1,\cdots,1}_{\xi-\ell-1} \Big)^{\mathsf{T}}, \quad \text{for } \ell = 1, 2, \ldots, \xi - 1, \quad \text{(B.1)}$$

and

$$\boldsymbol{w}_0^{(\ell,d_0^{(\ell)}(t))}(t) = \frac{1}{\xi}\Big(\underbrace{0,\cdots,0}_{n-t-1+\ell-\xi}, -\xi, \underbrace{0,\cdots,0}_{t-\ell}, \underbrace{1,\cdots,1}_{\xi} \Big)^{\mathsf{T}}, \quad \text{for } \ell = \xi, \xi + 1, \cdots, t.$$

The generalized left-eigenvectors are then given as follows. Let

$$\Omega_{t,\xi} := -\frac{t-\xi+1}{\xi}.$$

For $\ell = 1, 2, \ldots, \xi - 1$,

$$\boldsymbol{w}_0^{(\ell,d_0^{(\ell)}(t)-q)}(t) = \frac{1}{\xi}\Big(\underbrace{0,\cdots,0,}_{(t+1)\{d_0^{(\ell)}(t)-(q+1)\}} \underbrace{1,\cdots,1,}_{\ell} \quad 1-\xi, \quad \underbrace{1,\cdots,1,}_{t-\ell}$$

$$\underbrace{\Omega_{t,\xi},\cdots,\Omega_{t,\xi},}_{t+1}\underbrace{\Omega_{t,\xi}^2,\cdots,\Omega_{t,\xi}^2,}_{t+1}\cdots,\underbrace{\Omega_{t,\xi}^{q-1},\cdots,\Omega_{t,\xi}^{q-1},}_{t+1}\underbrace{\Omega_{t,\xi}^q,\cdots,\Omega_{t,\xi}^q}_{\xi}\Big)^{\mathsf{T}},$$

$q = 1, \ldots, d_0^{(\ell)}(t) - 1$. For $\ell = \xi, \xi + 1, \ldots, t$,

$$\boldsymbol{w}_0^{(\ell,d_0^{(\ell)}(t)-q)}(t) = \frac{1}{\xi}\Big(\underbrace{0,\cdots,0,}_{(t+1)\{d_0^{(\ell)}(t)-(q+1)\}+\ell} \quad -\xi, \quad \underbrace{0,\cdots,0,}_{t-\ell}\underbrace{1,\cdots,1,}_{t+1}$$

$$\underbrace{\Omega_{t,\xi},\cdots,\Omega_{t,\xi},}_{t+1}\underbrace{\Omega_{t,\xi}^2,\cdots,\Omega_{t,\xi}^2,}_{t+1}\cdots,\underbrace{\Omega_{t,\xi}^{q-1},\cdots,\Omega_{t,\xi}^{q-1},}_{t+1}\underbrace{\Omega_{t,\xi}^q,\cdots,\Omega_{t,\xi}^q}_{\xi}\Big)^{\mathsf{T}},$$

$q = 1, \ldots, d_0^{(\ell)}(t) - 1$.

Notice that $|\Omega_{t,\xi}| > 1$ if $1 \leq \xi < (t+1)/2$, and $|\Omega_{t,\xi}| < 1$ if $(t+1)/2 < \xi \leq t$. The exponential change by unit $t+1$ of the amplitude of $w_{0j}^{(\ell,d_0^{(\ell)}(t)-q)}(t)$ in $j \in \{1, 2, \ldots, n\}$ shows that the generalized left-eigenvectors represent *boundary pseudomodes* associated with the pseudospectrum including λ_0 [26, Section 7].

By (3.4), $\|\boldsymbol{v}_0^{(\ell,1)}(t)\| = \sqrt{2}$ independently of ℓ. And in the case $d_0^{(\ell)}(t) = \lfloor n/(t+1) \rfloor + 1$, $\|\boldsymbol{w}_0^{(\ell,d_0^{(\ell)}(t))}(t)\| = \sqrt{(\xi-1)/\xi} \leq \sqrt{(t-1)/t}$ independently of ℓ by (B.1). Therefore, for $d_0^{(\ell)}(t) = k_0(t) = \lfloor n/(t+1) \rfloor + 1$, $\kappa_0(t) = \sqrt{2(t-1)/t}$, and hence

$$t\kappa_0(t) = \sqrt{2t(t-1)}. \tag{B.2}$$

References

[1] Banks, J., Garza-Vargas, J., Kulkarni, A., Srivastava, N.: Pseudospectral shattering, the sign function, and diagonalization in nearly matrix multiplication time. Foundation of Computational Mathematics **23**, 1959–2047 (2023)

[2] Banks, J., Kulkarni, A., Mukherjee, S., Srivastava, N.: Gaussian regularization of the pseudospectrum and Davies' conjecture. Commun. Pure App. Math. **74**, 2114–2131 (2021)

[3] Basak, A., Paquette, E., Zeitouni, O.: Regularization of non-normal matrices by Gaussian noise – The banded Toeplitz and twisted Toeplitz cases. Forum of Mathematics, Sigma **7**, e3 (2019) (72 pages)

[4] Basak, A., Paquette, E., Zeitouni, O.: Spectrum of random perturbations of Toeplitz matrices with finite symbols. Trans. Amer. Math. Soc. **373** (7), 4999–5023 (2020)

[5] Basak, A., Zeitouni, O.: Outliers of random perturbations of Toeplitz matrices with finite symbols. Probab. Theory Relat. Fields **178**, 771–826 (2020)

[6] Böttcher, A., Silbermann, B.: Introduction to Large Truncated Toeplitz Matrices. Springer-Verlag, New York (1999)

[7] Bourgade, P., Cipolloni, G., Huang, J.: Fluctuations for non-Hermitian dynamics. arXiv:math.PR/2409.02902

[8] Bourgade, P., Dubach, G.: The distribution of overlaps between eigenvectors of Ginibre matrices. Probab. Theory Relat. Fields **177**, 397–464 (2020)

[9] Burda, Z., Grela, J., Nowak, M. A., Tarnowski, W., Warchoł, P.: Unveiling the significance of eigenvectors in diffusing non-Hermitian matrices by identifying the underlying Burgers dynamics. Nucl. Phys. B **897**, 421–447 (2015)

[10] Byun, S.-S., Forrester, P. J.: Progress on the Study of the Ginibre Ensembles. KIAS Springer Series in Mathematics 3, Springer (2024)

[11] Collingwood, D. H., McGovern, W. M.: Nilpotent orbits in semisimple Lie algebras. Van Nostrand Reinhold Mathematics Series, Van Nostrand Reinhold Co., New York (1993)

[12] Esaki, S., Katori, M., Yabuoku, S.: Eigenvalues, eigenvector-overlaps, and regularized Fuglede–Kadison determinant of the non-Hermitian matrix-valued Brownian motion. arXiv:math.PR/2306.00300

[13] Forrester, P. J.: Log-Gases and Random Matrices. Princeton University Press, Princeton, NJ (2010)

[14] Forrester, P. J.: Rank 1 perturbations in random matrix theory – A review of exact results. Random Matrices: Theory and Applications **12** (4) 2330001 (2023)

[15] Fyodorov, Y. V.: On statistics of bi-orthogonal eigenvectors in real and complex Ginibre ensembles: Combining partial Schur decomposition with supersymmetry. Commun. Math. Phys. **363**, 579–603 (2018)

[16] Gansner, E. R.: Acyclic digraphs, Young tableaux and nilpotent matrices. SIAM J. Alg. Disc. Meth. **2** (4), 429–440 (1981)

[17] Ginibre, J.: Statistical ensembles of complex, quaternion, and real matrices. J. Math. Phys. **6**, 440–449 (1965)

[18] Grela J., Warchoł, P.: Full Dysonian dynamics of the complex Ginibre ensemble. J. Phys. A: Math. Theor. **51**, 425203 (26 pages) (2018)

[19] Kato, T.: Perturbation Theory for Linear Operators. Springer-Verlag, Berlin, Corrected Printing of the Second Edition (1980)

[20] Katori, M.: Bessel Processes, Schramm–Loewner Evolution, and the Dyson Model. SpringerBriefs in Mathematical Physic, Vol. 11, Springer, Singapore (2016)

[21] Morimoto, S., Katori, M., Shirai, T.: Eigenvalue and pseudospectrum processes generated by nonnormal Toeplitz matrices with rank 1 perturbations. arXiv:math-ph/2401.08129

[22] Petrov, F. V., Sokolov, V. V.: Asymptotics of the Jordan normal form of a random nilpotent matrix. J. Math. Sci. **224** (2), 339–344 (2017)

[23] Reichel, L., Trefethen, L. M.: Eigenvalues and pseudo-eigenvalues of Toeplitz matrices. Linear Algebra Appl. **162–164**, 153–185 (1992)

[24] Sjöstrand, J. Vogal, M. Toeplitz band matrices with small random perturbations. Indagationes Mathematicae **32** (1), 275–322 (2021)

[25] Tao, T.: Outliers in the spectrum of iid matrices with bounded rank perturbations. Probab. Theory Relat. Fields **155**, 231–263 (2013)

[26] Trefethen, L. N., Embree, M.: Spectra and Pseudospectra: the Behavior of Nonnormal Matrices and Operators. Princeton University Press, Princeton (2005)